

MAGNETIC FORMING PROCESSES

by


MORIHIRO MYODO

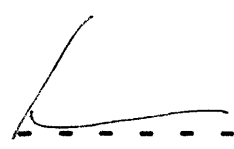
B.E. Keio Gijuku University
(1961)

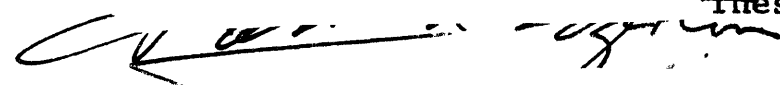
SUBMITTED IN PARTIAL FULFILLMENT OF THE
REQUIREMENTS FOR THE DEGREE OF
MASTER OF SCIENCE

at the

MASSACHUSETTS INSTITUTE OF TECHNOLOGY
June, 1963

Signature of Author 
Department of Electrical Engineering, May 17, 1963

Certified by 
Thesis Supervisor


Accepted by
Chairman, Departmental Committee on Graduate Students

MAGNETIC FORMING PROCESSES

by

Morihiro Myodo

Submitted to the Department of Electrical Engineering in June 1963 in partial fulfillment of the requirements for the degree of Master of Science.

ABSTRACT

Magnetic Forming is a relatively new method of high-energy-rate metal forming. In this thesis, limited details of the process were investigated. Such questions were considered as: What kind of coil gives the best results? How much energy is needed, and how can we determine the input parameters to maximize efficiency?

The theory of magnetic forming was studied, and experiments were carried out on sheet metal forming. The efficiencies were calculated as dependent upon power supply voltage and capacitance. The transients were observed on an oscilloscope during discharge, using a simulating circuit. The distinguishing features of the process and its possible uses were investigated. The cost was estimated for the set-up of the system.

Thesis Supervisor: Nathan H. Cook

Title: Associate Professor of Mechanical Engineering

Harold E. Edgerton

Professor of Electrical Measurements

ACKNOWLEDGEMENT

The author acknowledges his supervisors, Prof. Cook and Prof. Edgerton for their great assistance. Personally the author feels it must be written down that Prof. Simon Foner of the National Magnetic Laboratory of M.I.T. gave him useful information, and in the Strobo Laboratory, Mr. Bill Max Robert, technician, made the experiments possible. Gratitude must be also expressed toward the students and persons working in the Strobo Laboratory and the Material Processing Laboratory for their obvious and unobvious influences. The author wishes to thank Mr. C. C. Roberts, MAGNEFORM Sales, General Atomic Division, General Dynamics Corporation, who offered the materials on MAGNEFORM.

TABLE OF CONTENTS

	<u>Page</u>
ABSTRACT	ii
ACKNOWLEDGEMENT	iii
Introduction 1	1
Chapter One: Theory of Magnetic Forming	5
1-1. The distribution of magnetic field intensity for one turn coil	5
1-2. The principles to produce the magnetic force	14
1-3. The derivation of the efficiency of Magnetic Forming processes	22
Chapter Two: Experimental equipment	29
2-1. The design of the coils	29
2-2. Die	33
2-3. Switches	34
2-4. Power Supply	35
2-5. Condenser	35
2-6. System	36
Chapter Three: Experimental results	38
3-1. Experiments	38
3-2. The efficiency of Magnetic Forming Processes	40

	<u>Page</u>
3-3. The observation of the oscillation at the time of discharge	51
Chapter Four: The utility and feasibility of Magnetic Forming	55
4-1. The distinguished features of Magnetic Forming	55
4-2. Possible uses of Magnetic Forming	56
4-3. The cost of this method	57
APPENDIX I. The definition of terms	60
APPENDIX II. Tensile test of test pieces	62
APPENDIX III. Comment on the improvement of coil. .	65
BIBLIOGRAPHY	66

Introduction:

In high energy physics, coils for high-intensity pulsed magnetic fields are being used and strong mechanical force can be experienced in the high magnetic field. This force is not welcome in high field production, but can be useful for magnetic forming. If we look at a summary of high field production, we find that (see Table I)⁽¹⁾ many investigators have considered the problem of magnetic force on the mechanical construction and have actually been faced with the deformation of coils and protective materials.

TABLE I. Summary of high field production

Investigator		Method	Max H (gauss)	Useful volume(cc)
Kapitza	(1924)	Battery discharge	500 000	0.005
Kapitza	(1927)	Electromechanical impulse	320 000	2
Wall	(1926)	Capacitor discharge	450 000	0.5
Bitter	(1936)	Continuous	100 000	25
de Haas and Westerdijk	(1946)	Battery discharge	200 000	1
Shoenberg	(1950)	Capacitor discharge	90 000	3
Olsen	(1953)	Capacitor discharge	150 000	0.15
Myers	(1953)	Capacitor discharge	250 000	0.5
Furth and Waniek	(1956)	Capacitor discharge	600 000	0.1
Foner and Kolm	(1956)	Capacitor discharge	750 000	0.1

From Bibliography (1)

William S. Wilson and R. J. Schwinghamer (NASA)⁽²⁾

report on Magnetic Forming. Much descriptive information

is set forth. This is an entire survey of the history of Magnetic Forming at the present time. Very interesting pictures of tube expansion are shown in this report.

According to it, at the Marshal Space Center of NASA, a 240 000 joule capacitor bank called "Medusa" presently is being used for magnetic forming research and development.

A. P. Langlois, Convair Division General Dynamics Corp., San Diego, ⁽³⁾ investigated the feasibility of Magnetic Forming. He described the process of development in General Dynamics for this method.

In 1958, the General Atomic Division of General Dynamics demonstrated how magnetic "pinch effects" could be used to deform thin metal tubes at the Atoms for Peace Conference in Geneva. ⁽⁴⁾ He considered the induced EMF and flux linkages and applied this to swaging of tubes. He used permanent coils and expendable coils. From the economical point of view, he recommended expendable coils which cost 2-3¢ each for swaging operations. These expendable coils are destroyed in use. A few examples of flat-coil forming are described, using aluminum and aluminum alloys.

D. F. Brower, General Atomic Division, General Dynamics Corp. ^(5,6,7) has also worked in the field of Magnetic Forming. "MAGNEFORM", a commercial magnetic forming machine is now available from General Atomic Division, General

Dynamic Corporation. Six kilo-joules are stored in a volume of about four cubic feet. The pamphlets and application data show the application to swaging, assembly shaping, expanding tubing, and coining, shearing, forming or blanking. Swagings of tubes of .500" to 2" diameter and about .040" thickness are reported. The work materials are copper, aluminum and steel.

The Naval Research Laboratory⁽⁸⁾ is using magnetic forming to swage tubes - in this case connectors for coaxial cable, and has developed a new blowout switch that greatly improves its practicality.

Blowout switches connect six Cornell-Dubilier 14 microfarad condensers, arranged in parallel, with the swaging head. A 100,000 ampere current flows across the gap when triggered by an external spark.

Sonar Transducers use the same principle of utilizing the magnetic force. Sonar Transducers produce the shock waves underwater, using flat and spiral coils and thick aluminum sheets.

In this paper, the principle of magnetic forming were considered. The coil construction was similar to the Sonar Transducer with slight improvements. The efficiency of the sheet metal deformation was calculated using test pieces of

Aluminum 2024 T3, .020" and .032" thickness, yield strength 50 000 psi. The size of the test pieces was 3 1/2 " x 3 1/2 ". A die, with a hole 2" diameter, and 1/2" thickness was made of mild steel. The relation of the effective factors, capacitors and the voltage of power supply, was investigated for particular conditions. Hopefully, these can be extended to the general conditions.

It turns out to be most effective to increase the voltage of the power supply, when capacitor bank is the same. The efficiency is decreased when the capacitance is increased beyond a certain amount, when the voltage is held constant.

The voltage oscillation between the terminals of coil have been observed by the oscilloscope with and without a work piece present, using six volts power supply battery. The damping effect due to the work piece is apparently recorded on the picture. This experiment will be expected to simulate the actual high voltage system. (See Fig. 15 of the whole system of Magnetic Forming.)

Chapter One. Theory of Magnetic Forming

1-1. The distribution of magnetic field intensity for a one turn coil.

The distribution of magnetic field intensity for the idealized one-turn coil was calculated on the plane including the flat one-turn coil by considering the symmetry of the coil. It is assumed that the current flows in the geometrical line, or idealized conductor and the Biot-Savart law was applied. 1-1-1. The inside of the coil. (Cf. Fig. 1)

$$(1) \quad 0 < S < R, \quad 0 < \varphi < \frac{\pi}{2}$$

From the geometry of the triangle determined by Fig. 1 the following equations are derived.

$$\frac{\sin(\frac{\pi}{2} - \varphi)}{r} = \frac{\sin \theta}{\frac{R}{\cos \varphi} - S} \quad (1)$$

$$r^2 = R^2 + S^2 - 2SR \cos \varphi \quad (2)$$

$$dl = R d\varphi \quad (3)$$

The Biot-Savart law is applied:

in M.K.S. system,

$$dH = \frac{I}{4\pi} \times \frac{dl \sin \theta}{r^2} \quad (4)$$

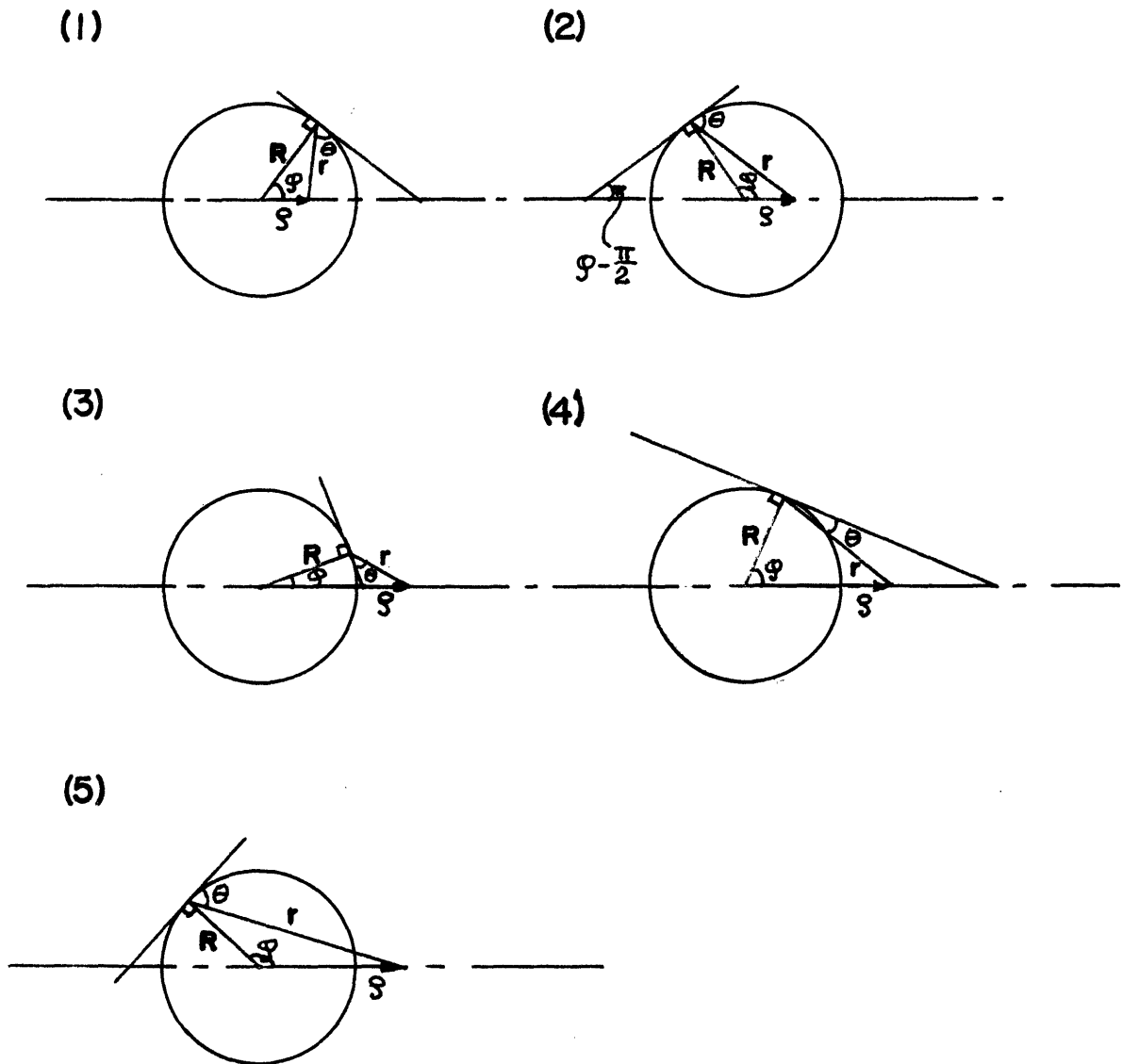


Fig.1 Cases of the calculation of field distribution

From the equation (1),

$$\sin \theta = \frac{l}{r} \times (R - s \cos \varphi) \quad (5)$$

This is combined with equation (4),

$$\begin{aligned} dH &= \frac{IR}{4\pi} \times \frac{l}{r^3} \times (R - s \cos \varphi) \\ &= \frac{IR^2}{4\pi} \times \frac{d\varphi}{r^3} - \frac{ISR}{4\pi} \times \frac{\cos \varphi}{r^3} d\varphi \end{aligned} \quad (6)$$

$$\frac{1}{2} H = \frac{IR^2}{4\pi} \times I_1 - \frac{ISR}{4\pi} \times I_2 \quad (7)$$

where $I_1 = \int_0^{\frac{\pi}{2}} \frac{d\varphi}{r^3}$ and $I_2 = \int_0^{\frac{\pi}{2}} \frac{\cos \varphi}{r^3} d\varphi$

From the equation (2),

$$r = \sqrt{R^2 + s^2 - 2SR \cos \varphi} \quad (8)$$

$$\begin{aligned} I_1 &= \int_0^{\frac{\pi}{2}} \frac{d\varphi}{(R^2 + s^2 - 2SR \cos \varphi)^{3/2}} \\ &= \frac{1}{(R^2 + s^2)^{3/2}} \int_0^{\frac{\pi}{2}} \frac{d\varphi}{\left(1 - \frac{2SR}{R^2 + s^2} \cos \varphi\right)^{3/2}} \end{aligned} \quad (9)$$

Let $\alpha = \frac{2SR}{R^2 + s^2}$ (10)

$$I_1 = \frac{1}{(R^2 + s^2)^{3/2}} \int_0^{\frac{\pi}{2}} \frac{d\varphi}{(1 - \alpha \cos \varphi)^{3/2}} \quad (11)$$

$$\text{Let } \beta = (1 - \alpha \cos \varphi)^{3/2} \quad (12)$$

$$\alpha \cos \varphi = 1 - \beta^{2/3} \quad (13)$$

$$\alpha \sin \varphi d\varphi = \frac{2}{3} \beta^{-1/3} d\beta \quad (14)$$

$$\alpha \sin \varphi = \beta^{1/3} \sqrt{2 - \beta^{2/3}} \quad (15)$$

$$d\varphi = \frac{2}{3} \times \beta^{-2/3} \times (2 - \beta^{2/3})^{-1/2} d\beta \quad (16)$$

$$I_1 = \frac{2}{3} \times \frac{1}{(R^2 + S^2)^{1/2}} \int_{(1-\alpha)^{1/2}}^1 \frac{d\beta}{\beta^{5/3} (2 - \beta^{2/3})^{1/2}} \quad (17)$$

$$\text{Let } \gamma = \beta^{1/3} \quad (18)$$

$$d\beta = 3\gamma^2 d\gamma \quad (19)$$

β	γ
1	1
$(1-\alpha)^{3/2}$	$(1-\alpha)^{1/2}$

$$I_1 = \frac{2}{(R^2 + S^2)^{1/2}} \int_{(1-\alpha)^{1/2}}^1 \frac{d\gamma}{\gamma^3 (2 - \gamma^2)^{1/2}} \quad (20)$$

$$= \frac{2}{(R^2 + S^2)^{1/2}} \left[-\frac{\sqrt{2 - \gamma^2}}{4\gamma^2} - \frac{1}{4\sqrt{2}} \log \frac{\sqrt{2} + \sqrt{2 - \gamma^2}}{\gamma} \right]_{(1-\alpha)^{1/2}}^1$$

$$I_2 = \int_0^{\frac{\pi}{2}} \frac{\cos \varphi}{r^3} d\varphi = \int_0^{\frac{\pi}{2}} \frac{\cos \varphi}{(R^2 + S^2 - 2SR \cos \varphi)^{3/2}} d\varphi \quad (21)$$

Using the equation (10) and (12),

$$I_2 = \frac{2}{\alpha(R^2 + S^2)^{1/2}} \int_{(1-\alpha)^{1/2}}^1 \frac{1 - r^2}{r^3 \sqrt{2 - r^2}} dr \quad (22)$$

$$I_2 = \frac{2}{\alpha(R^2 + S^2)^{1/2}} \left\{ \left[-\frac{\sqrt{2-r^2}}{4r^2} - \frac{1}{4\sqrt{2}} \log \frac{\sqrt{2} + \sqrt{2-r^2}}{r} \right]_{(1-\alpha)^{1/2}}^1 \right. \\ \left. - \left[-\frac{1}{\sqrt{2}} \log \frac{\sqrt{2} + \sqrt{2-r^2}}{r} \right]_{(1-\alpha)^{1/2}}^1 \right\} \quad (23)$$

$$(2) \quad 0 < \varphi < R, \quad \frac{\pi}{2} < \theta < \pi$$

$$r^2 = s^2 + R^2 - 2sR \cos \varphi \quad (24)$$

$$\frac{\sin(\varphi - \frac{\pi}{2})}{r} = \frac{\sin(\pi - \theta)}{\frac{R}{\cos(\pi - \varphi)} + s} \quad (25)$$

Equation (25) then becomes:

$$\sin \theta = \frac{1}{r} (R - s \cos \varphi) \quad (26)$$

This is the same as Equation (5). Therefore, the inside pattern of the coil is determined by the following equation:

$$H = \frac{IR^2}{\pi \alpha (R^2 + S^2)^{1/2}} \left[-\frac{\sqrt{2-r^2}}{4r^2} - \frac{1}{4\sqrt{2}} \log \frac{\sqrt{2} + \sqrt{2-r^2}}{r} \right]_{(1-\alpha)^{1/2}}^{(1+\alpha)^{1/2}} \\ - \frac{ISR}{\pi \alpha (R^2 + S^2)^{1/2}} \left\{ \left[-\frac{\sqrt{2-r^2}}{4r^2} - \frac{1}{4\sqrt{2}} \log \frac{\sqrt{2} + \sqrt{2-r^2}}{r} \right]_{(1-\alpha)^{1/2}}^{(1+\alpha)^{1/2}} \right. \\ \left. + \left[\frac{1}{\sqrt{2}} \log \frac{\sqrt{2} + \sqrt{2-r^2}}{r} \right]_{(1-\alpha)^{1/2}}^{(1+\alpha)^{1/2}} \right\} \quad (27)$$

1-1-2. The outside of the coil

$$(3) \quad S > R, \quad 0 < \varphi < \cos^{-1} \frac{R}{S}$$

$$r^2 = R^2 + S^2 - 2SR \cos \varphi \quad (28)$$

$$\frac{\sin(\frac{\pi}{2} + \varphi)}{r} = \frac{\sin \theta}{S - \frac{R}{\cos \varphi}} \quad (29)$$

The equation (29) is reduced:

$$\sin \theta = \frac{1}{r} \times (S \cos \varphi - R) \quad (30)$$

The direction of the magnetic field intensity is reversed.

$$-dH = \frac{I}{4\pi} \times \frac{R d\varphi \sin \theta}{r^2} = \frac{I}{4\pi} \times \frac{R(S \cos \varphi - R)}{r^3} d\varphi$$

$$dH = \frac{I}{4\pi} \times \frac{R(R - S \cos \varphi)}{r^3} d\varphi \quad (31)$$

This equation is of the same form to the equation (6):

$$(4) \quad S > R, \quad \cos^{-1} \frac{R}{S} < \varphi < \frac{\pi}{2}$$

$$r^2 = R^2 + S^2 - 2SR \cos \varphi \quad (32)$$

$$\frac{\sin \theta}{\frac{R}{\cos \varphi} - S} = \frac{\sin(\frac{\pi}{2} - \varphi)}{r} \quad (33)$$

The reduction of the equation (33) is:

$$\sin \theta = \frac{1}{r} \times (R - S \cos \varphi) \quad (34)$$

The equation (32) and (34) give the same form as equation (6).

$$(5) \quad S > R, \quad \frac{\pi}{2} < \varphi < \pi$$

$$r^2 = R^2 + S^2 - 2SR \cos \varphi \quad (35)$$

$$\frac{\sin(\frac{\pi}{2} - \theta)}{S} = \frac{\sin \varphi}{r} \quad (36)$$

$$\cos \theta = \frac{S}{r} \times \sin \varphi \quad (37)$$

$$\sin \theta = \frac{\sqrt{r^2 - S^2 \sin^2 \varphi}}{r} \quad (38)$$

$$\begin{aligned} dH &= \frac{I}{4\pi} \times \frac{R d\varphi \sin \theta}{r^2} = \frac{I}{4\pi} \times \frac{d\varphi}{r^2} \times \frac{\sqrt{r^2 - S^2 \sin^2 \varphi}}{r} \\ &= \frac{IR}{4\pi} \times \frac{d\varphi}{r^3} \times \sqrt{R^2 + S^2 - 2SR \cos \varphi - S^2 \sin^2 \varphi} \\ &= \frac{IR}{4\pi} \times \frac{d\varphi}{r^3} \times \sqrt{S^2 \cos^2 \varphi - 2SR \cos \varphi + R^2} \\ &= \frac{IR}{4\pi} \times \frac{d\varphi}{r^3} \times (R - S \cos \varphi) \end{aligned} \quad (39)$$

This is the same form to the equation (6)

(6) $S = 0$, the center of the coil.

$$dH = \frac{I}{4\pi} \times \frac{R d\varphi}{R^2} = \frac{I}{4\pi R} d\varphi \quad (40)$$

$$H = \frac{I}{4\pi R} \int_0^{2\pi} d\varphi = \frac{I}{2R} \quad (41)$$

The total result:

$$\frac{2RH}{I} = -\frac{2}{\pi} \times \frac{I_A}{\left[1 + \left(\frac{S}{R}\right)^2\right]^{3/2}} - \frac{1}{\pi} \times \frac{I_B}{\left[1 + \left(\frac{S}{R}\right)^2\right]^{3/2}} \quad (42)$$

$$\text{where } I_A = -\frac{(1+\alpha)^{3/2} - (1-\alpha)^{3/2}}{4(1-\alpha^2)} + \frac{1}{4\sqrt{2}} \log \frac{1-\alpha + \sqrt{2(1-\alpha)}}{1+\alpha + \sqrt{2(1+\alpha)}} \quad (43)$$

$$I_B = \frac{(1+\alpha)^{3/2} - (1-\alpha)^{3/2}}{4(1-\alpha^2)} + \frac{3}{4\sqrt{2}} \log \frac{1-\alpha + \sqrt{2(1-\alpha)}}{1+\alpha + \sqrt{2(1+\alpha)}} \quad (44)$$

$$\alpha = \frac{2SR}{R^2 + S^2}$$

S/R	$2RH/I$
0.0	1.000
0.1	0.127
0.2	0.250
0.3	0.371
0.4	0.496
0.5	0.627
0.6	0.762
0.7	0.960
0.8	1.270
0.9	2.300
1.0	-----
1.1	-1.300
1.2	-0.240
1.3	-0.170
1.4	-0.100
1.5	-0.066
1.6	-0.038
1.7	-0.028
1.8	-0.019
1.9	-0.015
2.0	+0.002 --- This should be negative.

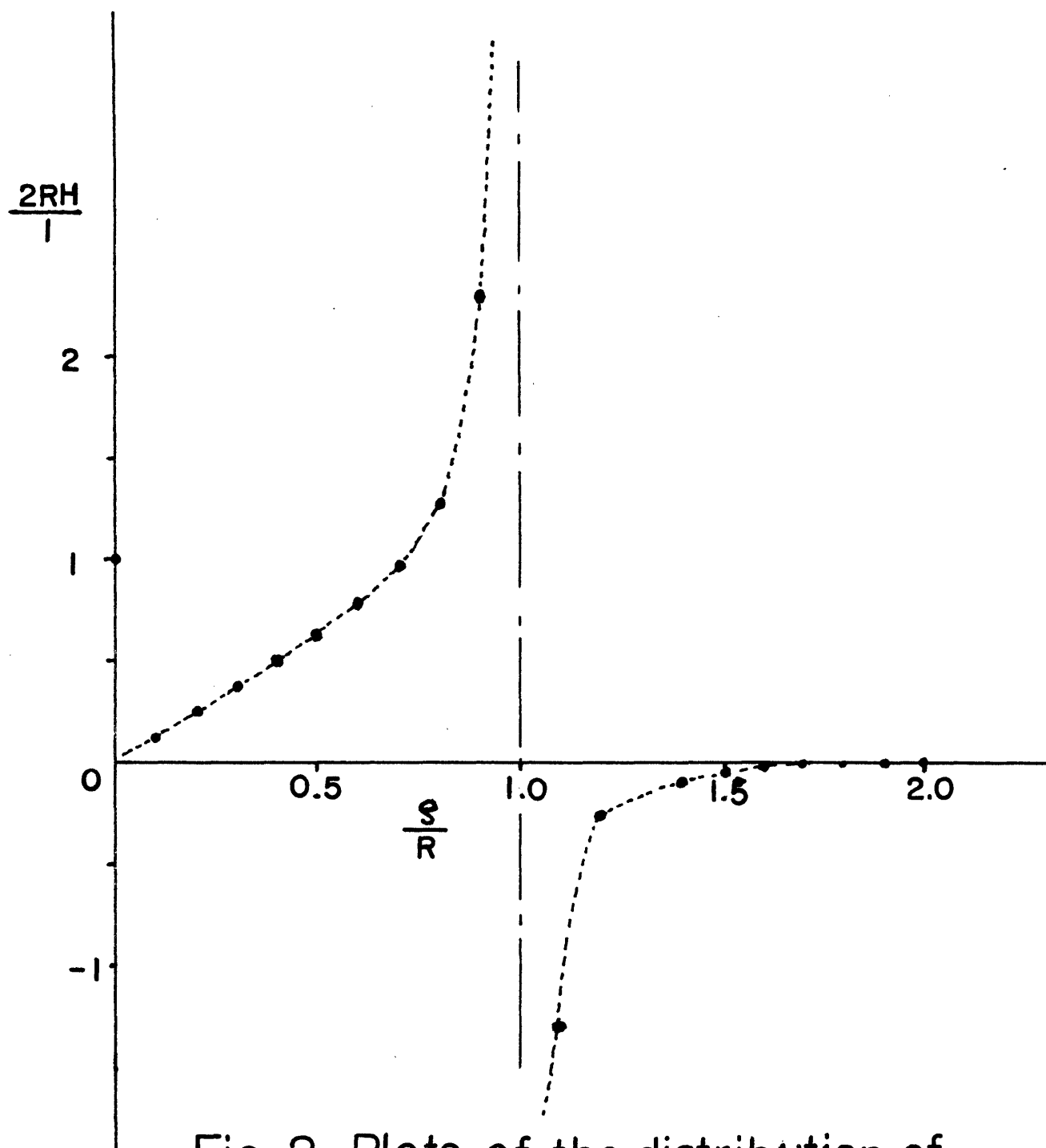


Fig. 2 Plots of the distribution of magnetic field intensity for one turn coil

We have idealized the current here. Now we must consider the difference between the idealized current and the actual current. We can understand it by the comparisons of the following examples.

The magnetic field of the current I flowing through the infinite straight wire without mass in free space is expressed by the following equation which represents the magnitude of H at the distance r away from the wire.

$$H = \frac{I}{2\pi r} \text{ (AT/m)} \quad (45)$$

If the wire is an infinite straight line and massive, as a wire of radius a , the magnitude of the magnetic field at the point at a distance r is:

$$H_o = \frac{I}{2\pi r} \quad r > a \quad (46)$$

$$\oint H dQ = 2\pi r H_i = \frac{I}{\pi a^2} \times \pi r^2 \quad (47)$$

$$H_i = \frac{I}{2\pi a^2} \times r \quad r < a \quad (48)$$

where the conductor is non-magnetic like a copper wire, the medium is air, and the current distribution is uniform across the area. These results were plotted in Fig. 3 and Fig. 4.

1-2. The principles of magnetic force production.

In Fig. 15 the Capacitor discharges the stored energy

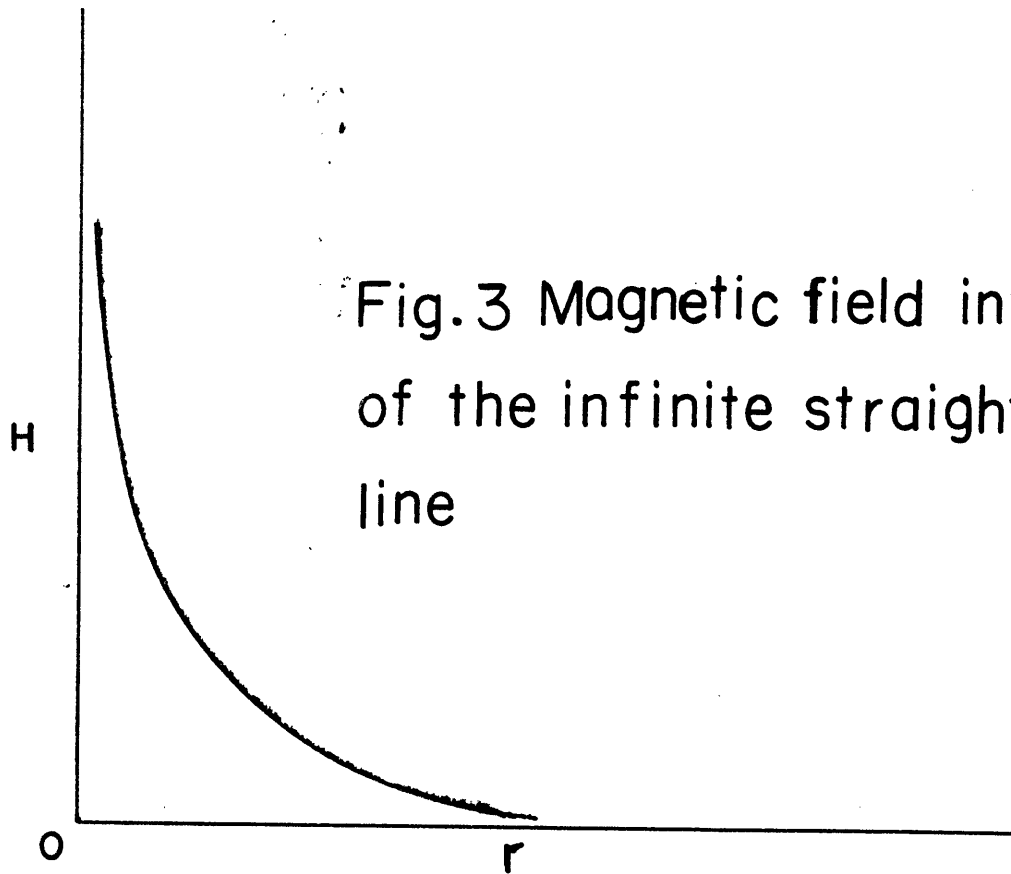


Fig.3 Magnetic field intensity of the infinite straight line

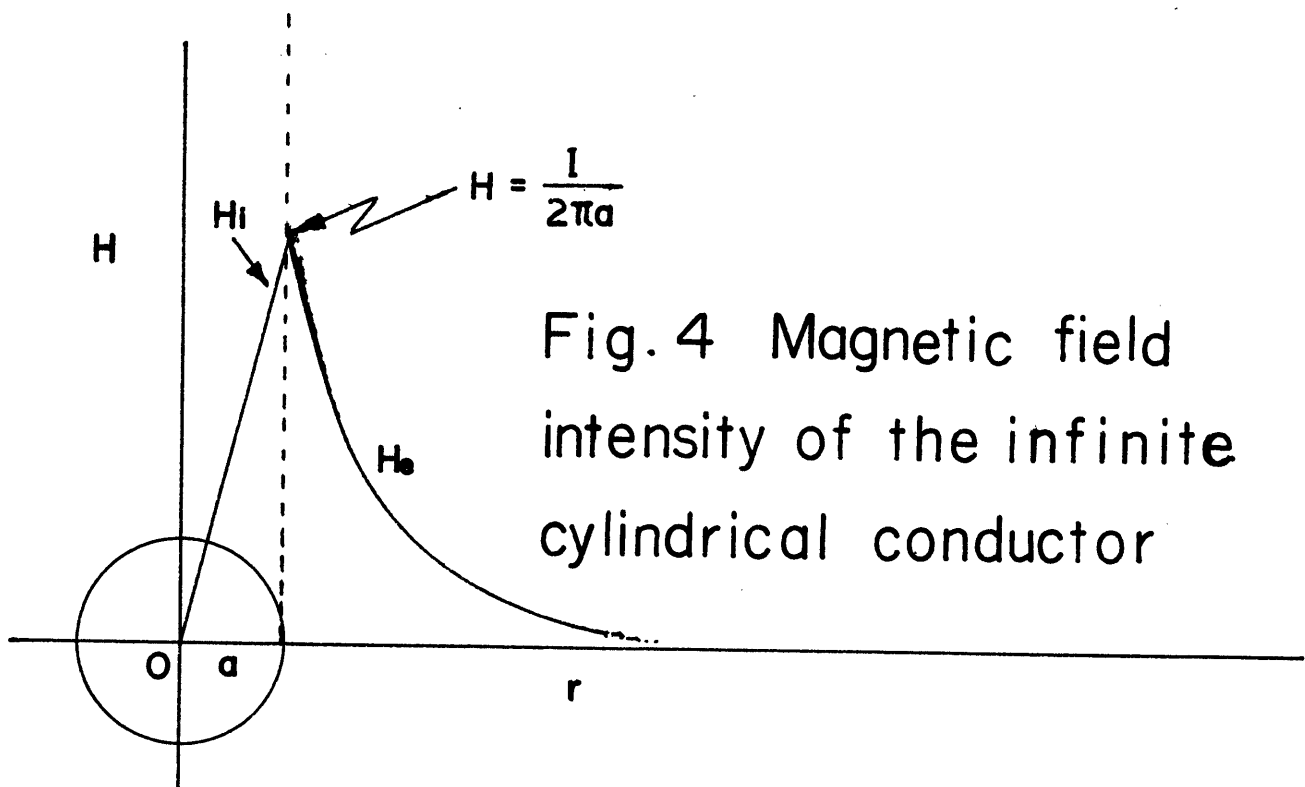


Fig.4 Magnetic field intensity of the infinite cylindrical conductor

through the coil or Transducer. The magnetic flux interlinks with the sheet or tube to produce magnetic forming. According to the electromagnetic induction law, if there is a secondary circuit very close to the primary circuit, a current will be induced in the secondary circuit when the magnitude of the primary current changes. This was originally discovered by Farady. Lenz's law determines the direction of the induced current, and Neumann's law is the statement regarding the magnitude of the induced voltage. Lenz's law:

When the flux inside the circuit changes, an electromotive force is induced in a direction such as to prevent the flux from changing.

Neumann's law for the electromagnetic induction:

The e.m.f. induced in the one-turn circuit, is equal to the decreasing rate of the interlinked flux.

$$e = - \frac{d\Phi}{dt} \quad (49)$$

$$\text{where } \Phi \text{ (magnetic flux)} = \int_s \mathbf{B} d\mathbf{S} = \int_s \mu \mathbf{H} d\mathbf{S}$$

$$\mathbf{B} \text{ (magnetic field density)} = \mu \text{ (permeability)} \cdot \mathbf{H} \text{ (magnetic field intensity)}$$

$$[\Phi] = [\text{Volt} \cdot \text{Second}] = [\text{Weber}]$$

$$[H] = [A \cdot T/m]$$

$$[B] = [Wb \cdot \text{Turn} / m^2]$$

$$[\mu] = [B/H] = [\text{Weber}/\text{Ampere} \cdot \text{meter}] = [\text{henry}/\text{meter}]$$

$$= \frac{4\pi}{10^9} = 1.257 \times 10^{-6} \text{ henry/meter}$$

The General expression of electro-magnetic induction's law:

$$\oint_c \mathbf{E} d\mathbf{Q} = - \frac{d}{dt} \int_s \mathbf{B}_n d\mathbf{s} = - \frac{d\Phi}{dt} \quad (50)$$

This is the integral form. The differential form is as follows:

$$\text{rot } \mathbf{E} = - \frac{\partial \mathbf{B}}{\partial t} \quad (51)$$

The current density in the conductor is:

$$\mathbf{i} = k\mathbf{E}, \text{ where } k \text{ is conductivity.} \quad (52)$$

If there is no conductor, \mathbf{E} and \mathbf{H} are propagated in free space at the velocity of light.

$$\nabla^2 \mathbf{E} = \varepsilon\mu \frac{\partial^2 \mathbf{E}}{\partial t^2} + \kappa\mu \frac{\partial \mathbf{E}}{\partial t} \quad (53)$$

$$\nabla^2 \mathbf{H} = \varepsilon\mu \frac{\partial^2 \mathbf{H}}{\partial t^2} + \kappa\mu \frac{\partial \mathbf{H}}{\partial t} \quad (54)$$

The propagation velocity is:

$$v = \frac{1}{\sqrt{\epsilon\mu}} \quad \text{m/sec} \quad (55)$$

In vacuum,

$$\frac{1}{\sqrt{\epsilon_0\mu_0}} = \sqrt{\frac{4\pi c^2}{10^7} \times \frac{10^7}{4\pi}} = c \doteq 3 \times 10^8 \quad \text{m/sec}$$

The conductor in which the current flows is influenced by the magnetic field from the outside, and experiences a passive force. This electromagnetic force is:

$$dF = I [d\ell \times B] = [i \times B] dv \quad (56)$$

The electromagnetic induction law states that the induced current flows in the reverse direction from the outside current producing the field. The following examples will give the better understanding concerning the interacting forces.

Examples:

(1). Two parallel straight conductors.

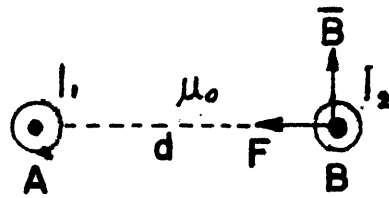
From Fig. 5, two infinite parallel straight lines are forced to be repulsed or to be mutually attracted, depending on the direction of the currents I_1 and I_2 .

$$\bar{B} = \frac{\mu_0 I}{2\pi d} \quad \text{at the point of B.}$$

$$F_0 \text{ (per unit length)} = \frac{\mu_0}{2\pi} \times \frac{1}{d} \times I_1 I_2 \quad \text{(Newton)} \quad (57)$$

Therefore, in the length l ,

(a)



(b)

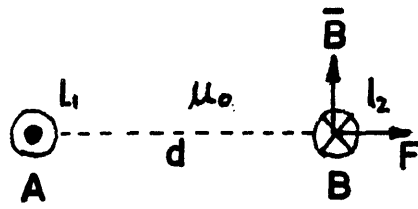


Fig.5 Forces interacting on parallel wires

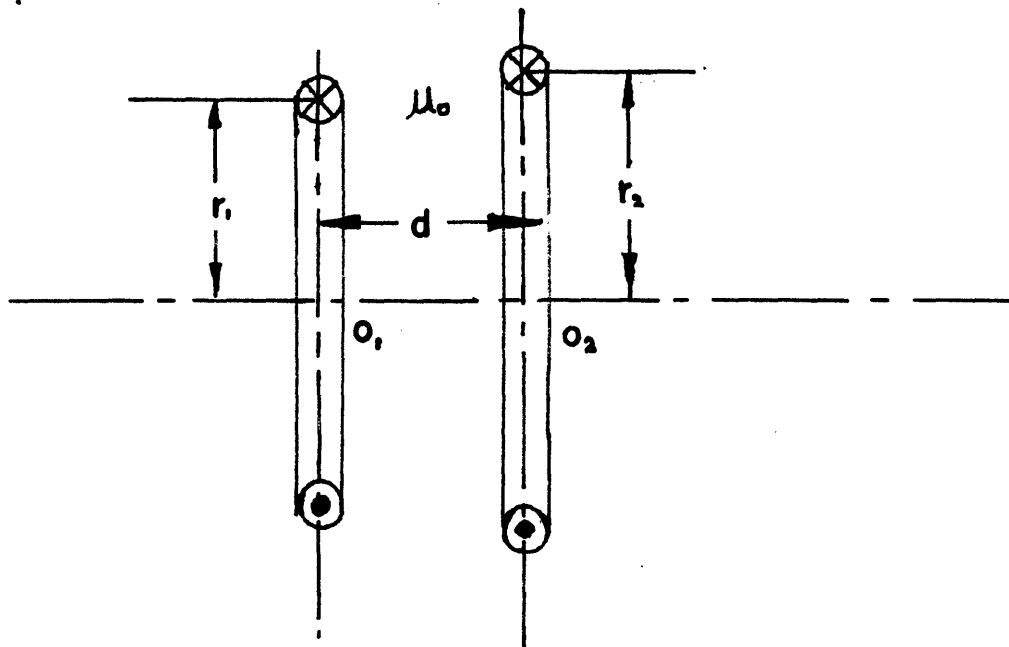


Fig.6 Two circular one-turn coils

$$F = \frac{\mu_0}{2\pi} \times \frac{l}{d} \times I_1 I_2 \quad (58)$$

This force is mutually attractive when the current flows in the same direction, and is repulsive when the currents flow in opposite directions.

(2) The force acting between the two close coils of wire on the same axis:

From Fig. 6 the circular current I_1 and I_2 at the radii r_1 and r_2 have an axial separation d ; and, if $d \ll r_1, r_2$, we can assume the two circular coil to act as two parallel conductors. Therefore, the approximate force acting on a segment dl of the other circuit is:

$$dF = \frac{\mu_0 I_1 I_2 dl}{2\pi \sqrt{d^2 + (r_2 - r_1)^2}} \quad (59)$$

The total force is:

$$F = \int_c \frac{d}{\sqrt{d^2 + (r_2 - r_1)^2}} dF = \frac{1}{2} \times \frac{\mu_0 (r_2 + r_1) d}{d^2 + (r_2 - r_1)^2} I_1 I_2 \quad (60)$$

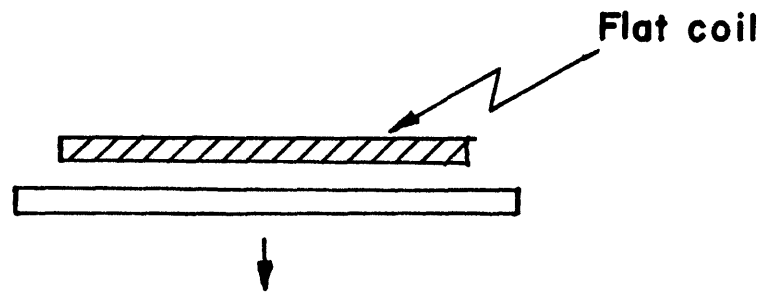
where both of the circumference are $\pi(r_1 + r_2)$

Particularly, if $r_1 = r_2 = a$,

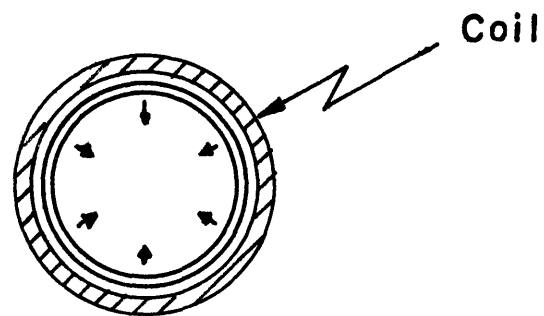
$$F = \frac{\mu_0 a}{d} \times I_1 I_2 \quad (61)$$

(Bibliography 9)

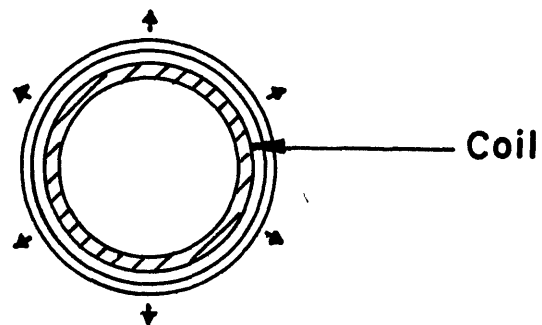
Now we can understand the produced force, when the



(a) Pressing operation



(b) Swaging operation



(c) Expansion of the tube

Fig. 7 Typical Magnetic Forming

capacitor bank is discharged. Magnetic forming is illustrated in Fig. 7 for the possible operations. If the reader considers the distribution of the magnetic field intensity for the one-turn coil, these illustrated operations are obvious, especially for (b) and (c) in Fig. 7.

1-3. The derivation of the efficiency for magnetic forming processes:

We will discuss the flat-sheet deformation. The test pieces and the die are specified as follows:

Table II. Specifications.

Test piece	size.	3 1/2" x 3 1/2"
	A1. 2024 T3	.020" Thickness .032" Thickness
	Yield Strength	50 000 psi
The die	Material:	mild steel
	Shape:	Fig. 8

In this case, the die has a hole of two inches diameter, therefore the work-piece undergoes free-deformation in this central part. We can now consider the energy required for deformation. The following method is owing to Mr. Jonathan Gestetner (Bibliography 13).

When a specimen is deformed, it assumes a certain shape. This was approximately fitted to be part of a sphere. The

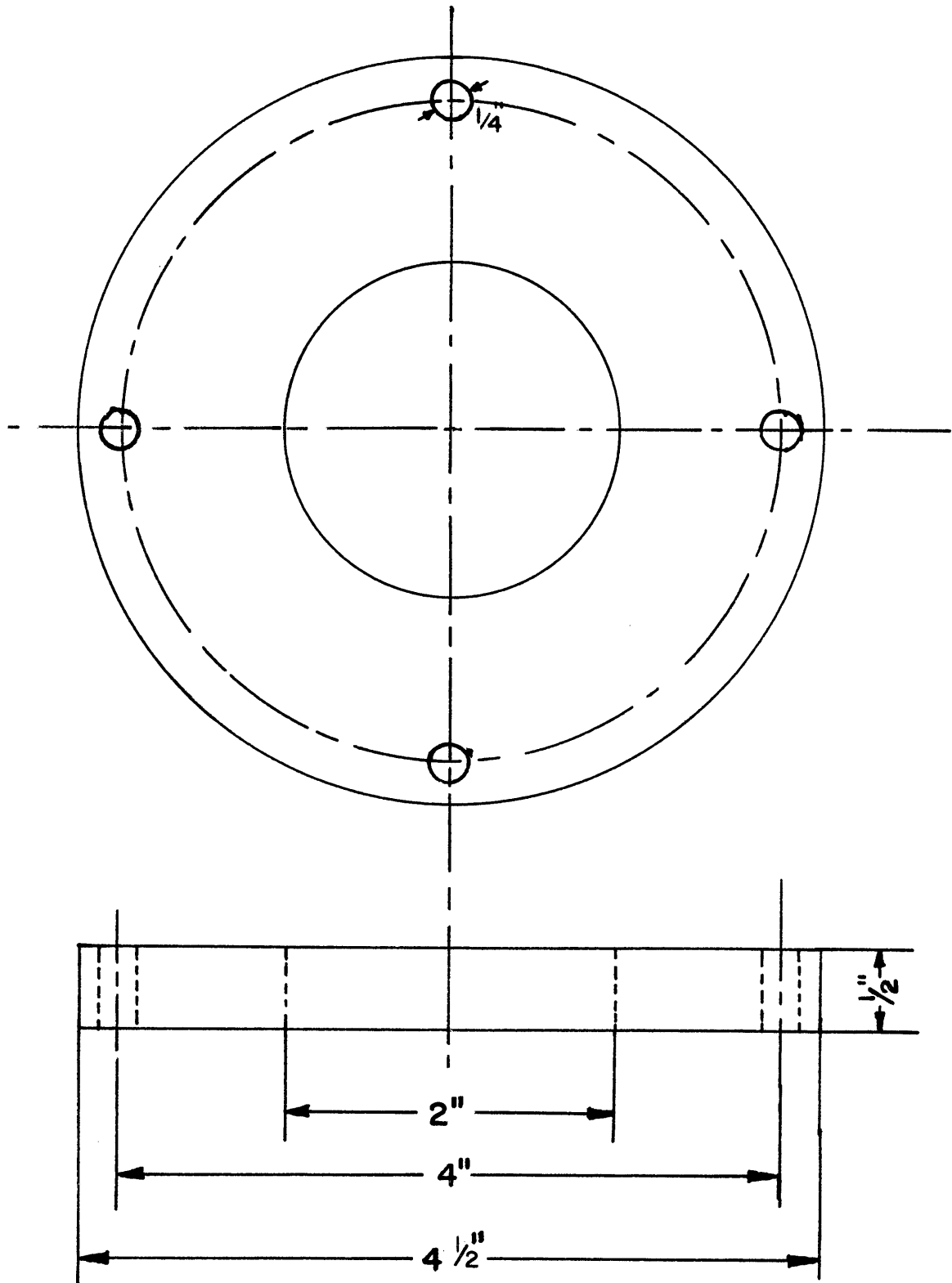


Fig. 8 Die

assumption will be made that the strain is uniform all over the deformed part of the specimen.

$$u = \int \sigma d\epsilon \quad (62)$$

u : the energy/vol. of metal
 σ : stress
 ϵ : strain

Assuming a stress-strain curve of Fig. 9 for the ductile material (Cf. Appendix I. Figs. 28, 29).

$$u = \sigma_0 \epsilon_h \quad (63)$$

$$\epsilon_h = \frac{A - A_0}{A_0} = \frac{A}{A_0} - 1 \quad (64)$$

A : final surface area of specimen

A_0 : surface area of underformed specimen

The area of the curved surface of a spherical segment of height h, radius of sphere r is $2\pi rh$. The radius of the sphere r is determined as follows: From Fig. 10 we have known the radius R of the die and can measure the depth of h.

$$H + h = r \quad (65)$$

$$H^2 + R^2 = r^2$$

$$\therefore r = \frac{h^2 + R^2}{2h}$$

$$A_0 = \pi R^2 \quad (66)$$

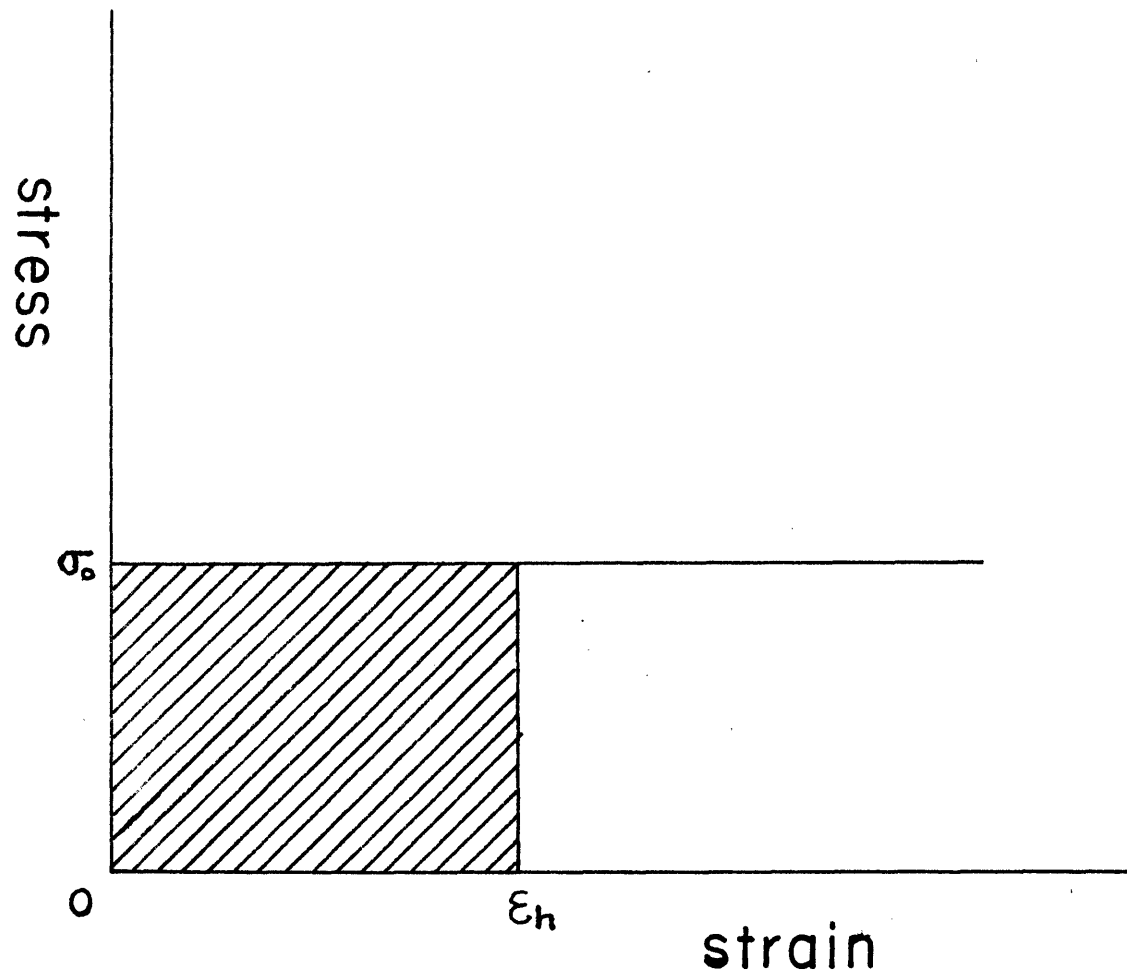


Fig.9 Assumed stress-strain
curve

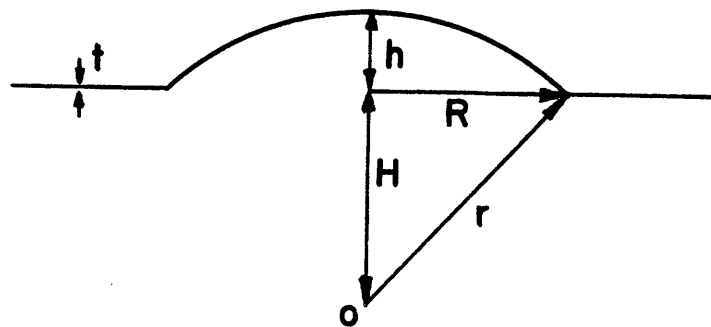


Fig.10 The figure of the deformation

$$A = 2\pi rh = \pi(h^2 + R^2) \quad (67)$$

$$\epsilon_h = \frac{A - A_0}{A_0} = \frac{h^2}{R^2} \quad (68)$$

$$\bar{U} = (\text{volume}) \times u = (\pi R^2 t) \times \sigma_0 \epsilon_h \quad (\text{in.}\cdot\text{lb}) \quad (69)$$

\bar{U} : total deformation energy in specimen of circular sheet deformation

t: the thickness of the work-piece

The equation (69) is reduced as follows:

$$\bar{U} = \pi R^2 t \sigma_0 \times \frac{h^2}{R^2} \quad (\text{in.}\cdot\text{lb}) \quad (70)$$

In this paper, $R = 1$ (in.)

The initial stored energy in Capacitor is:

$$U = \frac{1}{2} C V^2 \quad (\text{watt}\cdot\text{sec}) \quad (71)$$

Table III. The units.

Ton(long) (tn.1) (U.S. or British)
= 2240 pounds (avoirdupois)

1 Joule (absolute) = 0.73756 foot-pound
= 8.85072 in.-lb.

1 foot = 12 inches

Watt-Second = Joule

The efficiency is calculated as follows:

From the equation (70) and (71),

$$\text{Effy.} = \frac{\bar{U}}{U} \times 100 \quad \% \quad (72)$$

The units of U and \bar{U} should be coherent.

Chapter Two: Experimental Equipments

2-1. The design of coils.

(1) Flat coil.

Coils similar to the Sonar Transducer were considered. Copper wire of square cross section was used. A comparison between the coil with a hole (Coil I) and the coil filled to the center with copper wire was made. (Cf. Fig. 11 and 12). The experiments show that the coil without a hole was better for magnetic forming.

Table IV. Coil Constructions

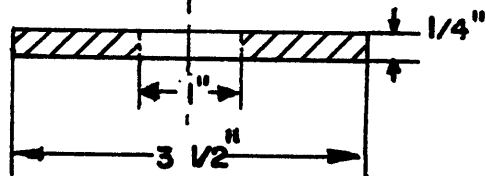
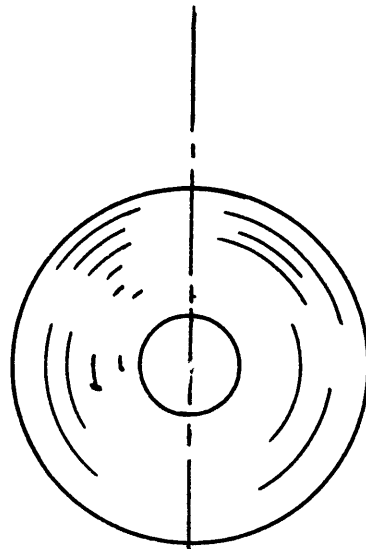
	O.D.	I.D.	Turns
Coil I	3 1/2"	1"	19
Coil II	3"	0"	24

Wire which was used: Copper wire of 1/4" x 1/16" rectangular cross-section wrapped by paper and insulated with Epoxy after the coil winding was completed.

(2) Helical coil.

This coil is suitable for swaging and expansion of tubes. Practically, it has a good construction for making and mechanical strength. This coil is being used in the National Magnetic Laboratory of M.I.T. ⁽¹⁾ This is a flat

Coil I
O.D. $3 \frac{1}{2}$ "
I.D. 1"
19 Turns



Coil II
O.D. 3"
I.D.
24 Turns

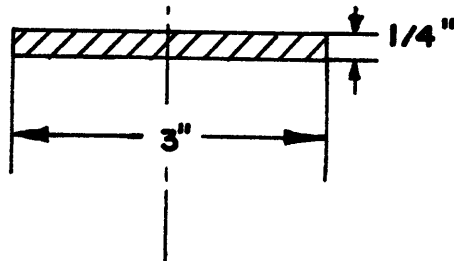
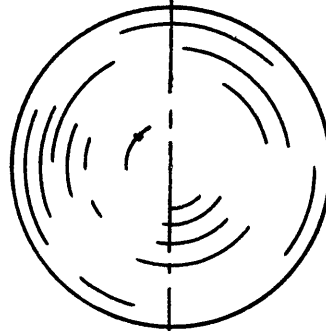


Fig. II Coil I and Coil II

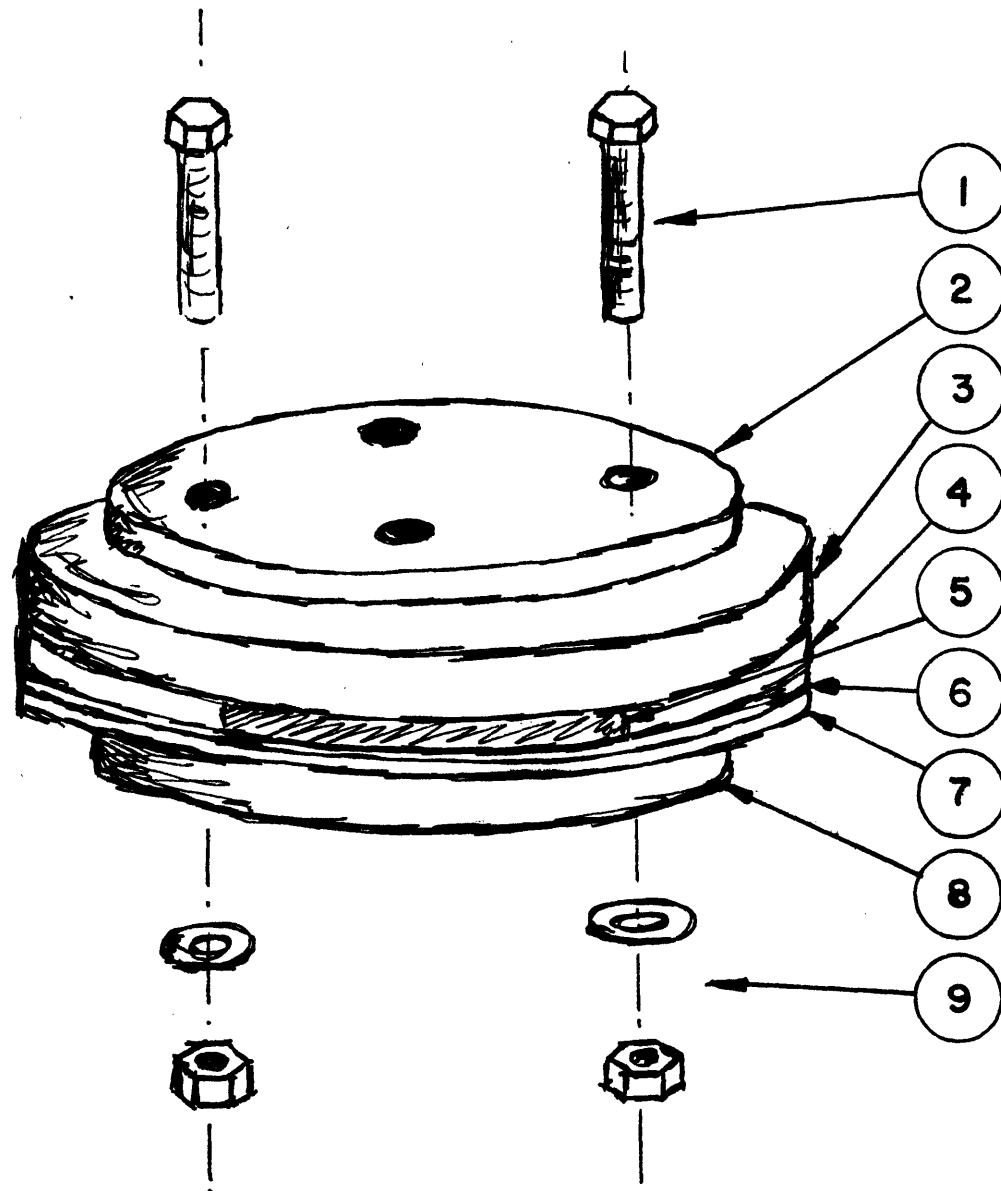


Fig. 12 Experimental construction of flat coil = 1. steel bolts 2. mild steel plate for mechanical strength 3. Bakelite insulator 4. Epoxy 5. magnetic coil 6. thin Bakelite sheet 7. work piece 8. die of mild steel 9. steel washer and nut

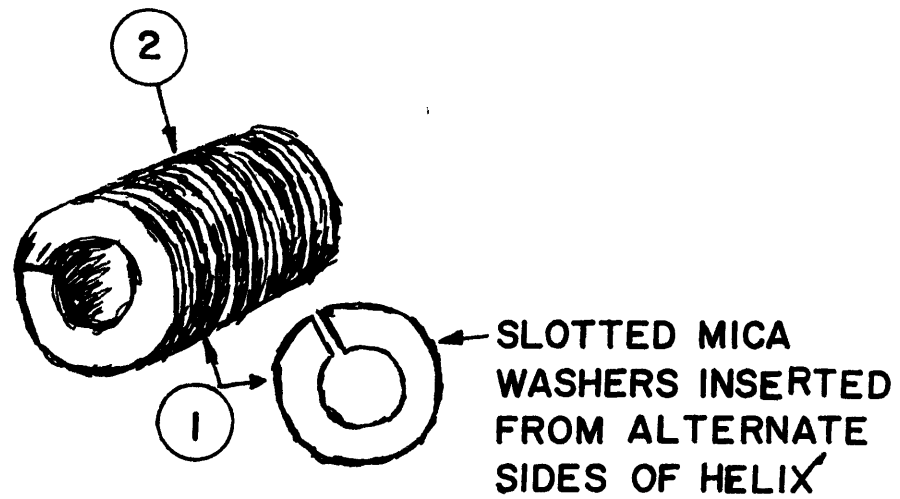


Fig.13 Helical coil = 1. mica 2. magnet
coil machined continuous spiral of beryllium-copper

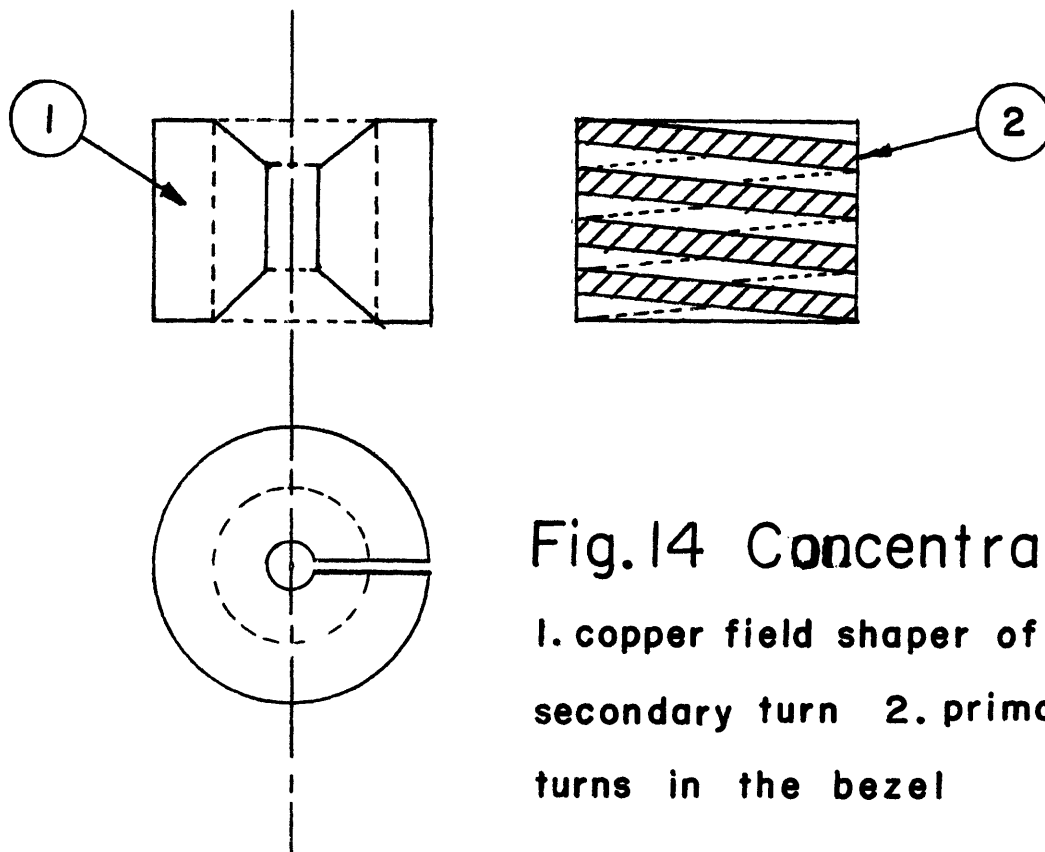


Fig.14 Concentrator

1. copper field shaper of
secondary turn 2. primary
turns in the bezel

helix of beryllium-copper, insulated between turns by two helices of mica and surrounded by a reinforced structure of ceramic. (Cf. Fig. 13).

(3) Concentrator.

This is suitable for swaging. It has many primary turns and single secondary turn. Concentrator is made of copper. The primary turns consist of wire inserted into a vinyl tube. (Cf. Fig. 14).

(4) Usual coil and expendable coil.

If it is carefully treated for mechanical strength, it will be available for magnetic forming. Expendable coils are of the same principle to the other coils but are wound directly on the tubes. This coil is very convenient and effective for the swaging service.

As to the material for the wire, copper is available and gives good results at room temperature. Silver is better for low resistance losses but is expensive and brittle. Superconductors are not available at the room temperature, at least, not now.

2-2. Die.

The die depends on the end use. Generally speaking, mild steel or silicon steel, and insulator like Bakelite or wood are available. Higher resistance materials are

best for the die material.

TABLE V. Resistivity

$$R = \rho \times \frac{L}{A} \quad (\text{ohm})$$

C 1018 Steel (mild)	= 14.3×10^{-6} ohm-cm
Al. 2024 T4	= 5.75×10^{-6} ohm-cm
Copper	= $1.71-2.03 \times 10^{-6}$ ohm-cm

2-3. Switches.

(1) Air gap switch.

An air gap with triggering circuit can be used. This is suitable for the repetitive use. The circuits for the safety and trigger make the system complex. This is widely used by adjusting the gap distance and has a long life.

(2) Knife edge switch.

Each blade of the high AC current switch (for about 300 A) which I used was available for experiment. In the sense of practical use, it is not so convenient, but the circuit is simplified for the temporary use.

(3) Ignitron.

This is used in "MAGNEFORM". The ignitron for discharge service is available from General Electric Company. For instance, GL-7171; 35 000 Amperes peak and 10 000 Volts peak,

GL-7703; 100 000 Amperes peak and 20 000 Volts peak. This information is offered for the technical rating. There is a rating limitation.

The air gap switch and the knife edge switch are usually noisy, when they are closed in capacitor discharge service.

2-4. Power-Supply.

The experiments show that higher DC voltage of the power supply gives better results. At least, it will be necessary to be above 4 kv. In this paper the power supply was varied up to 10 kv. It is limited by the maximum rating of capacitor peak DC voltage and the allowable maximum current of power supply and time constant. The power supply for higher voltages is usually equipped with safety circuits.

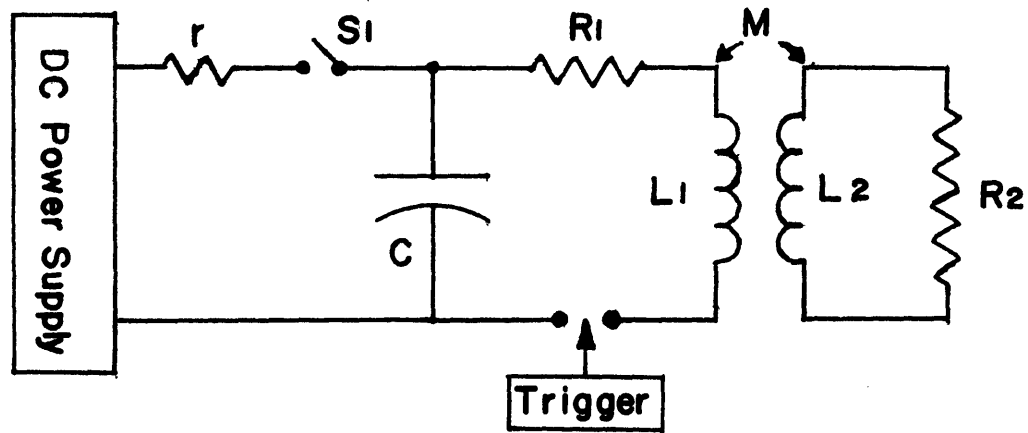
2-5. Capacitor.

Electric discharge capacitors of higher peak DC voltage ratings are available. According to Simon Foner and Henry H. Kolm,⁽¹⁾ the fact that it allows current backswing has not caused any capacitor failure after several thousand discharges, both in 20 kv and 3 kv systems. Normal operation of metal forming can be experimented with from 1000 joules up. For instance, a 4 kv power supply and 166 mfd give 1328 joules; 7 kv power supply and 42 mfd give 1029 joules.

2-6. System.

The system is composed of a high voltage power supply and high energy storage. Humans must be protected by safety circuits and instruments. If one needs to touch the discharge capacitors directly in operation, the capacitors must be short-circuited by an appropriate tool. The complete power supply and triggering circuits must be packaged very carefully. Figure 15 is the simplified functional diagram of the magnetic forming system.

The procedure of magnetic forming is as follows:
The switch S1 of power supply is closed. Capacitor C then stores the energy. S1 is opened and the Trigger operated. The energy of the capacitor is discharged through the coil or Transducer. The work piece deforms by the magnetic force.



C = total capacitor

r = current-limiting resistance

R_1 = total resistance of coil & connector

L_1 = inductance of coil

R_2 = effective resistance of work piece

L_2 = effective inductance of work piece

M = effective mutual inductance

Fig.15 System diagram

Chapter Three: Experimental Results

3-1. Experiments.

3-1-1. Pressing.

Using the before-mentioned die, flat Coil I and II, and the test pieces, the experiments have been done. Firstly, fixing the power supply voltage at 4 kv, the capacitor bank was increased. The range of the stored energy is about 600 watt-second to 6000 watt-second. Secondly, fixing the capacitor bank at 42 mfd, the power supply voltage is varied from 4 kv to 10 kv. In each case, the maximum depth was measured and the efficiency was calculated. (Cf. Fig. 16).

If the test piece is non-conductive or high resistive material, for example, steel, it makes magnetic forming very difficult. It seems to me that even steel is impossible for direct magnetic forming. The experiment done with steel proves this statement. The experimental set-up was the power supply voltage of 4 kv and the stored energy about 6000 watt-second. The following method made the pressing of steel possible. The soft Aluminum sheet, thickness .016" near the coil was attached to the steel test piece (.016" thickness, Yield Strength 90 000 psi). The obvious pressing could be recognized. The set-up was the power supply voltage 4 kv and the initially stored energy

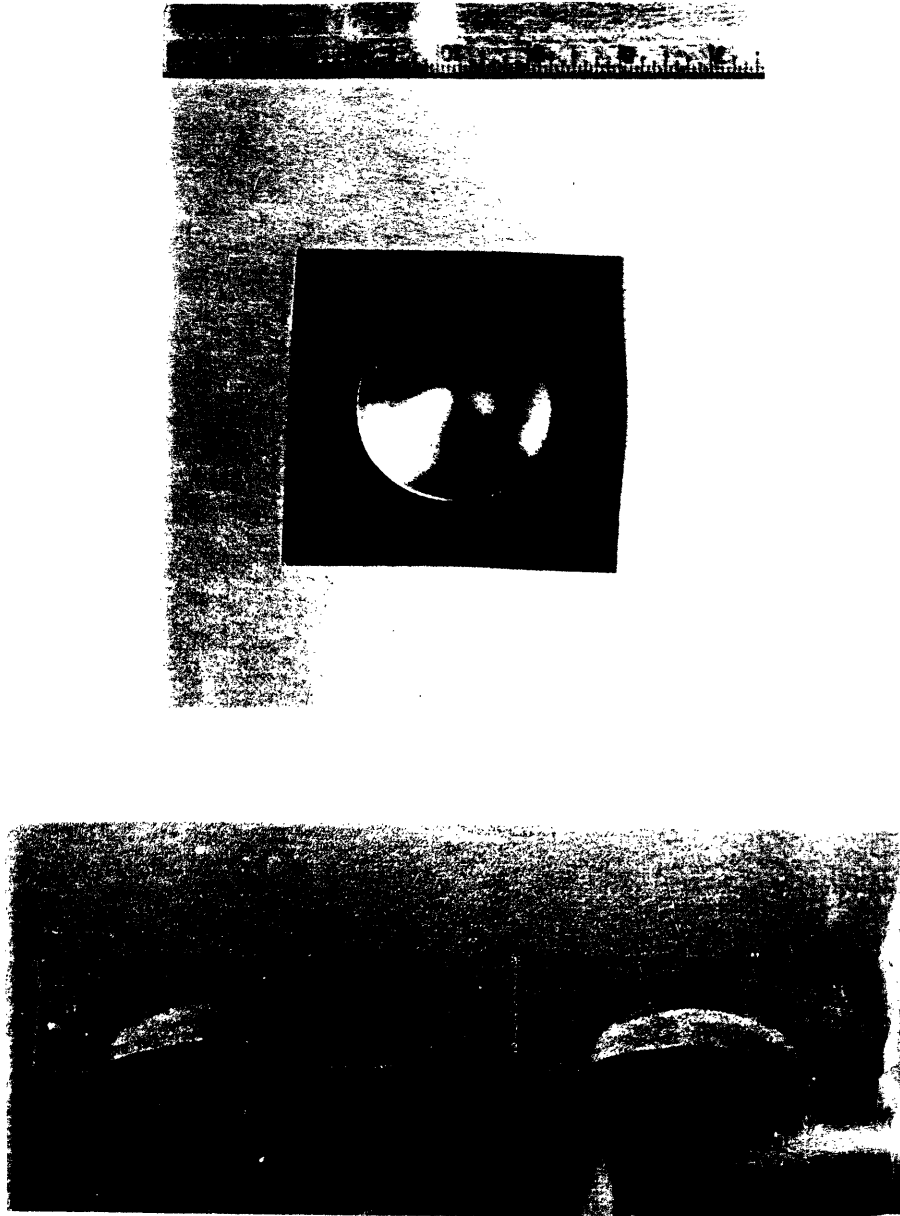


Fig.16 Deformed work piece

about 6000 watt-second.

When this experiment was conducted, the Aluminum sheet became hot, because the high current was induced and the energy was consumed.

3-1-2. Swaging.

As the subsidiary experiment, swaging, using the expendable coil, was carried out. The tube was about 1" diameter, soft Aluminum .016" thickness. The insulated wire was wound directly on the tube, about five or six turns. The experimental set-up is the power supply voltage 4 kv and the stored energy 1 328 joule. The swaging could be obviously recognized.

3-1-3. Lettering.

The complex pattern is possible to copy on the thin Aluminum sheet, using magnetic force.

As the die, the wood which the letters was graved was used. The thin copper and soft Al. sheet, about .016" thickness, 3 1/2" x 3 1/2" was experimented. The power supply voltage and the stored energy were 4 kv and 1328 Joule, using Coil II. Figure 17 shows the lettering by magnetic pressing.

3-2. The Efficiency of Magnetic Forming Processes.

The experimental data of the pressing (Cf. 3-1-1) is as follows:



Fig. 17 Lettering (Embossing)

Experiment I:

Coil I, Number of discharges 1

Power supply voltage 4 kv

Work piece Al. 2024 T3 .020" thickness

Stored energy watt-second	Efficiency %	Depth h in.
664	0.8	0.121
1328	0.8	0.175
1992	0.4	0.152
2656	0.5	0.191
3320	0.5	0.198
3984	0.4	0.206
4648	0.3	0.191
5312	0.3	0.207
5976	0.2	0.183
6640	0.2	0.182

Experiment II:

Coil I, Number of discharges 1

Power supply voltage 4 kv

Work piece Al. 2024 T3 .032" thickness

Stored energy watt-second	Efficiency %	Depth h in.
664	.05	.070
1328	.7	.124
1992	.4	.124
2656	.5	.148
3320	.4	.148
3984	.3	.156
4648	.3	.148
5312	.3	.163
5976	.2	.148
6640	.2	.163

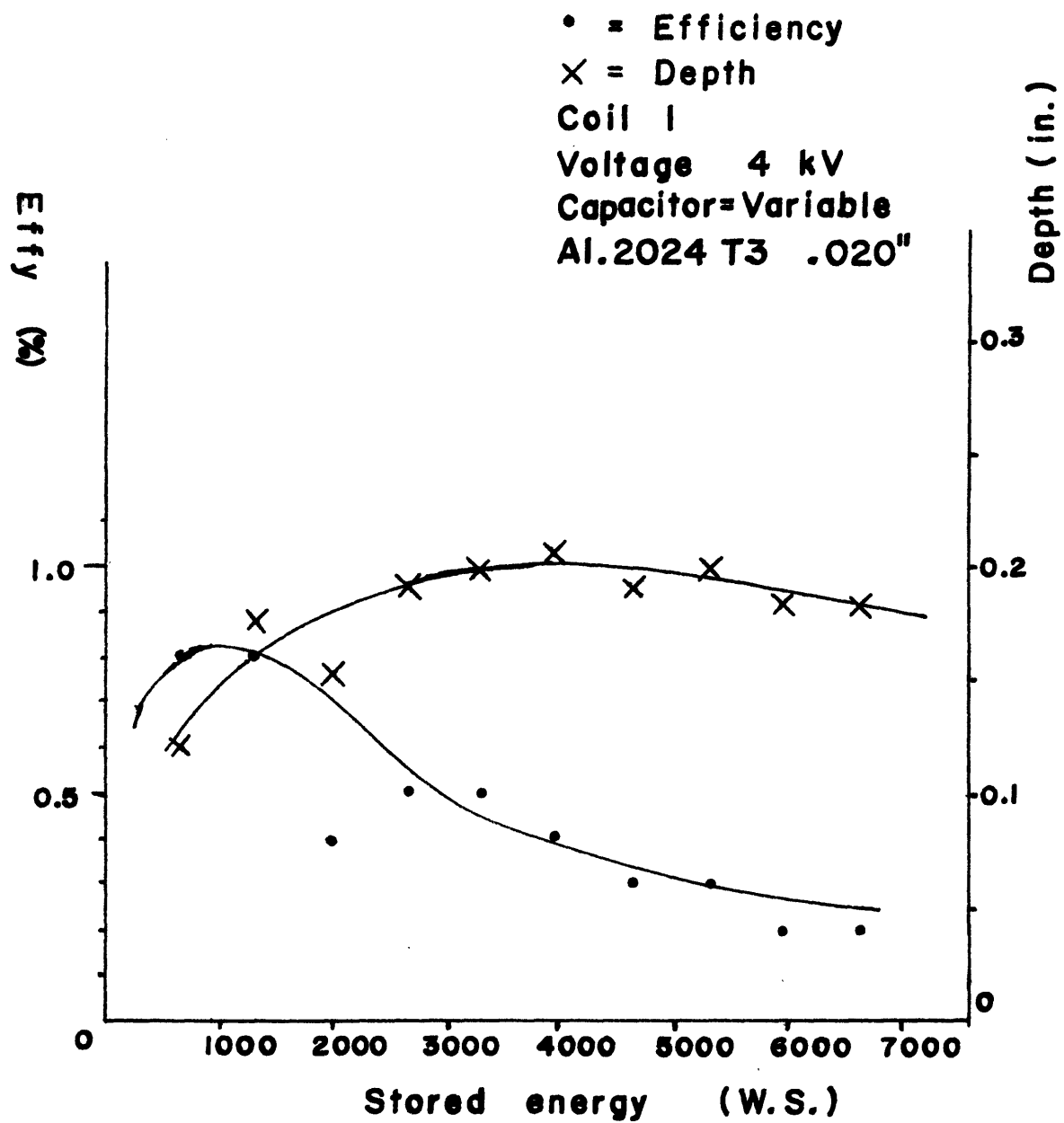


Fig.18 Experiment I

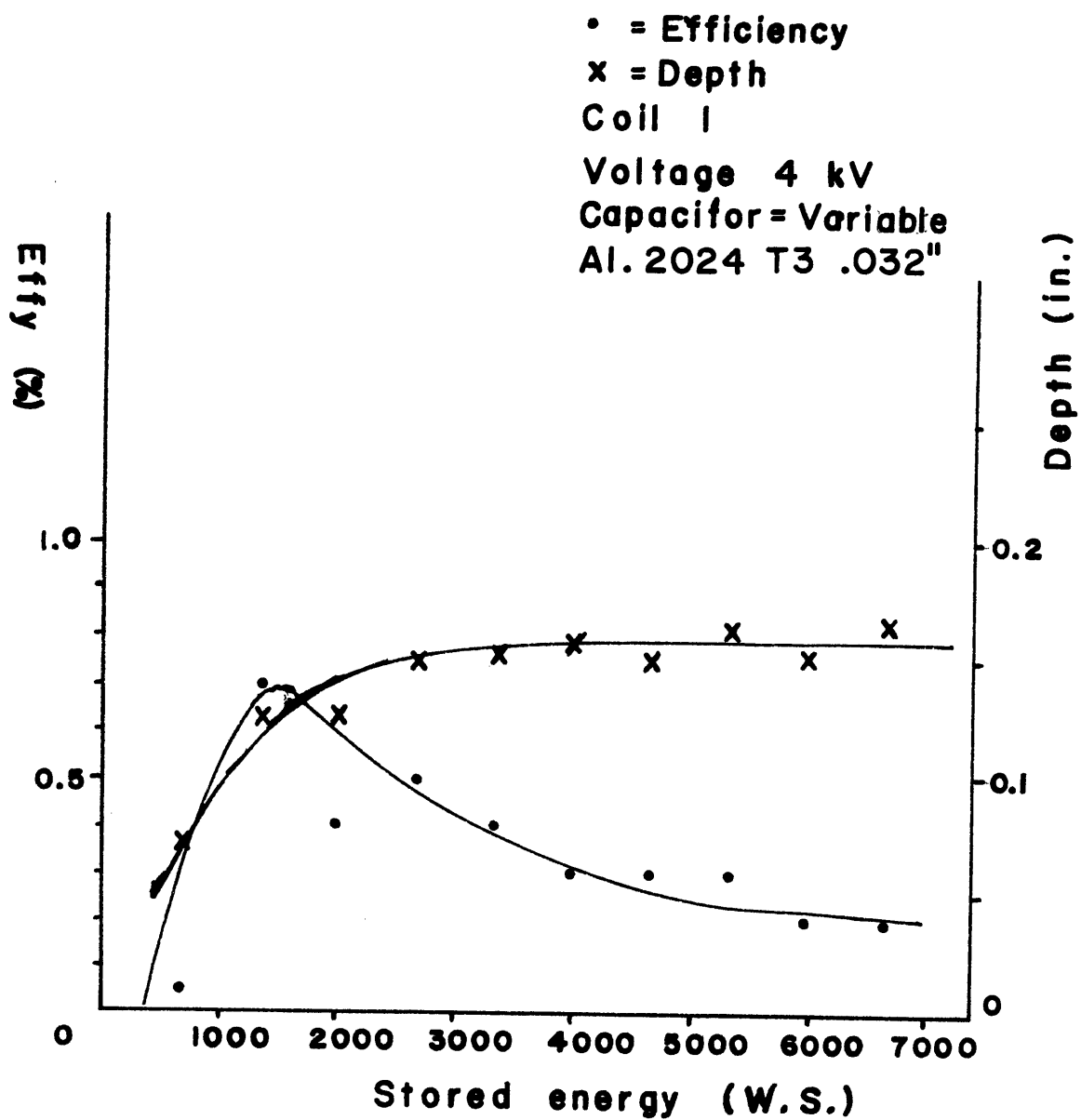


Fig. 19 Experiment II

Experiment III:

Coil II, Number of discharges 1

Power supply voltage 4 kv

Work piece Al. 2024 T3 .020 thickness

Stored energy watt-second	Efficiency %	Depth h in.
664	2.0	0.191
1328	2.0	0.268
1992	1.2	0.261
2656	1.2	0.293
3320	0.8	0.268
3984	0.8	0.284
4648	0.5	0.261
5312	0.6	0.308
5976	0.5	0.277
6640	0.5	0.292

Experiment IV:

Coil II. Number of discharges 1

Power supply voltage 4 kv

Work piece Al. 2024 T3 .032 thickness

Stored energy watt-second	Efficiency %	Depth h in.
664	1.4	0.124
1328	2.0	0.218
1992	1.3	0.210
2656	1.4	0.257
3320	0.9	0.234
3984	0.9	0.249
4648	0.5	0.210
5312	0.7	0.249
5976	0.5	0.226
6640	0.6	0.257

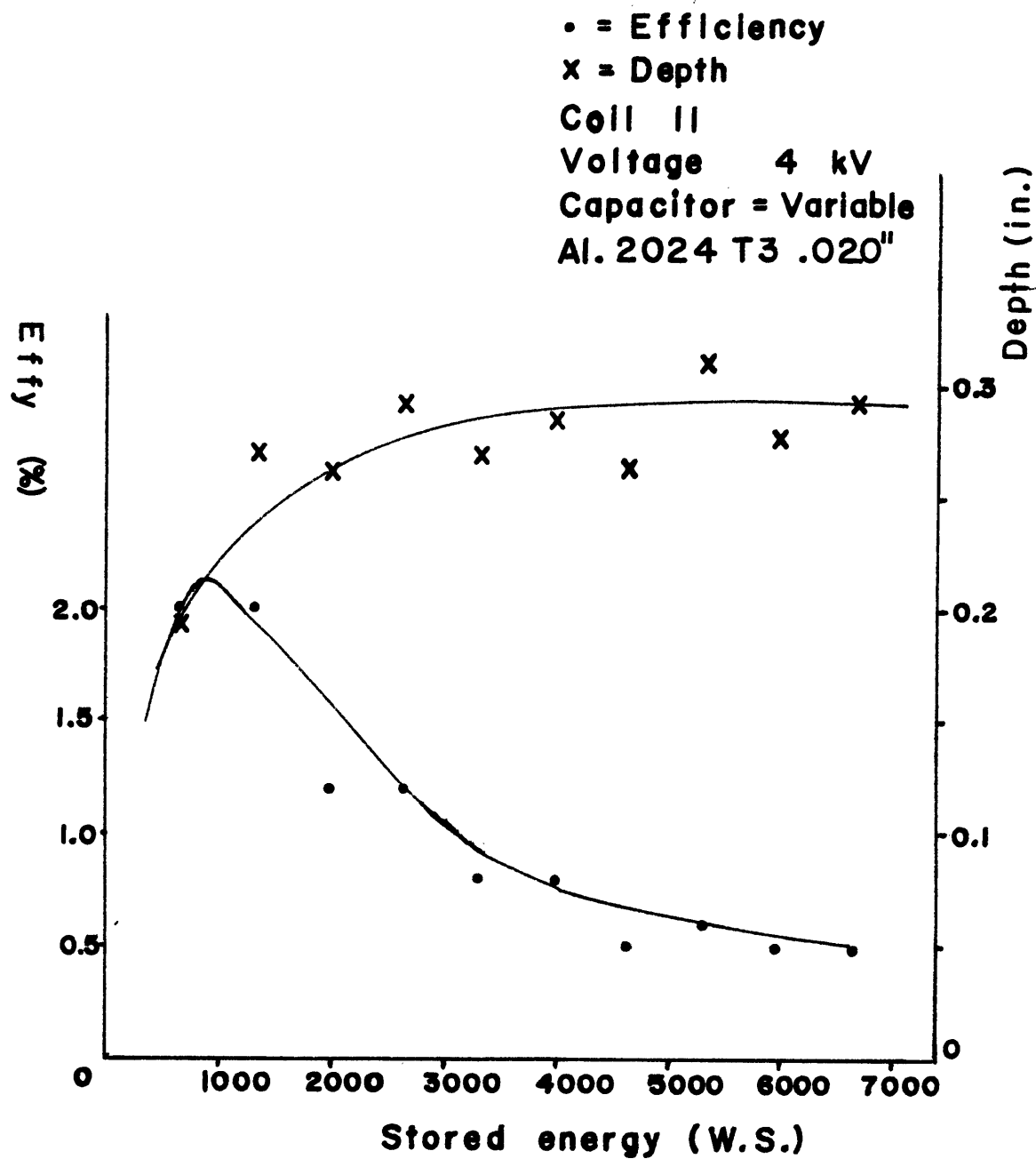


Fig. 20 Experiment III

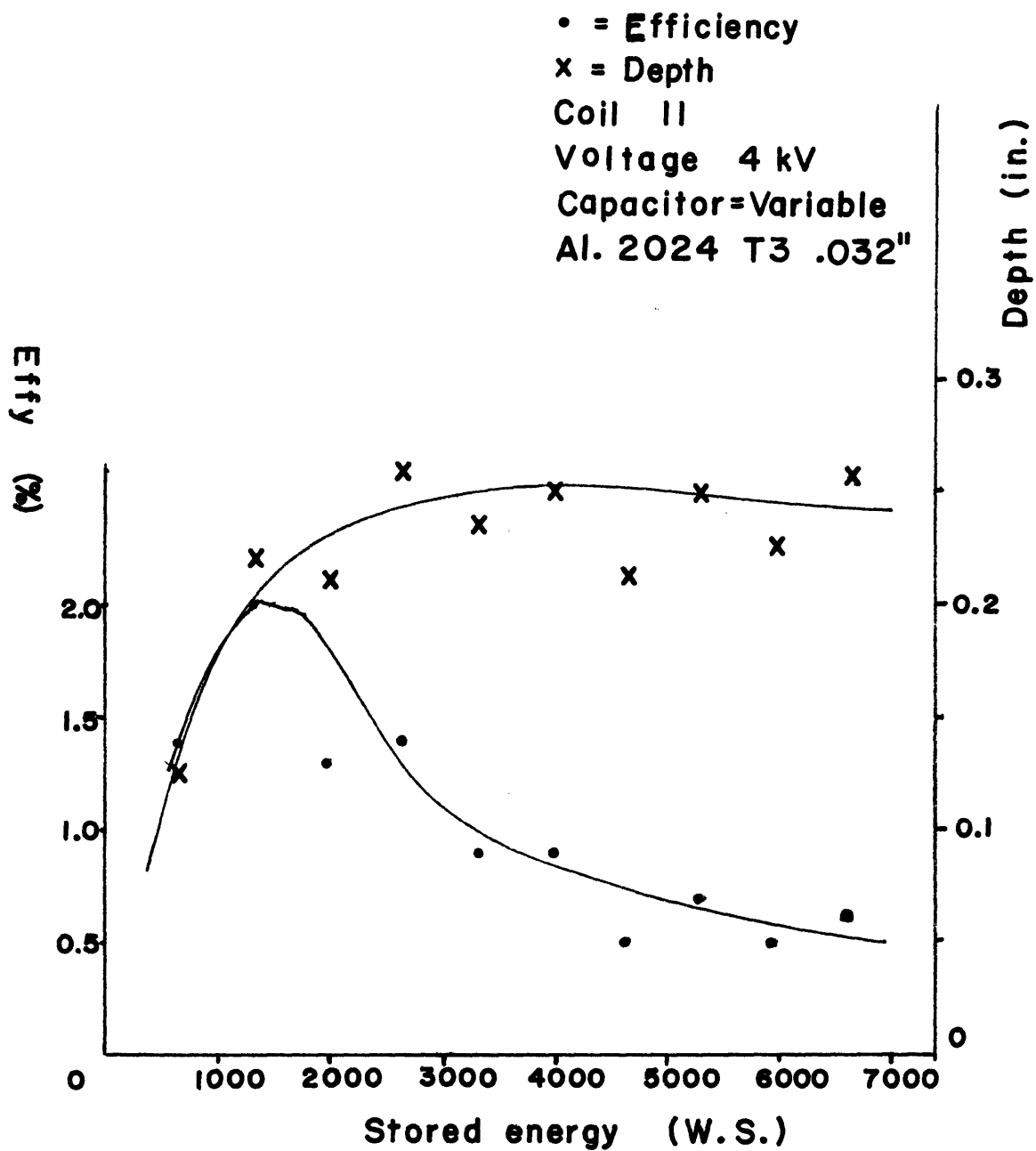


Fig. 21 Experiment IV

Experiment V:

Coil II, Number of discharges 1

Capacitor 42 mfd

Work piece Al. 2024 T3 .020" thickness

Stored energy watt-second	Efficiency %	Depth h in.
336	1.2	0.105
525	2.1	0.175
756	2.8	0.246
1029	3.3	0.308
1344	3.6	0.371
1701	3.9	0.433
2100	4.2	0.496

Experiment VI.

Coil II, Number of discharges 1

Capacitor 42 mfd

Work piece Al. 2024 T3 .032" thickness

Stored energy watt-second	Efficiency %	Depth h in.
336	0.6	0.062
525	1.3	0.109
756	2.4	0.179
1029	3.0	0.234
1344	3.3	0.281
1701	3.9	0.343
2100	4.1	0.390

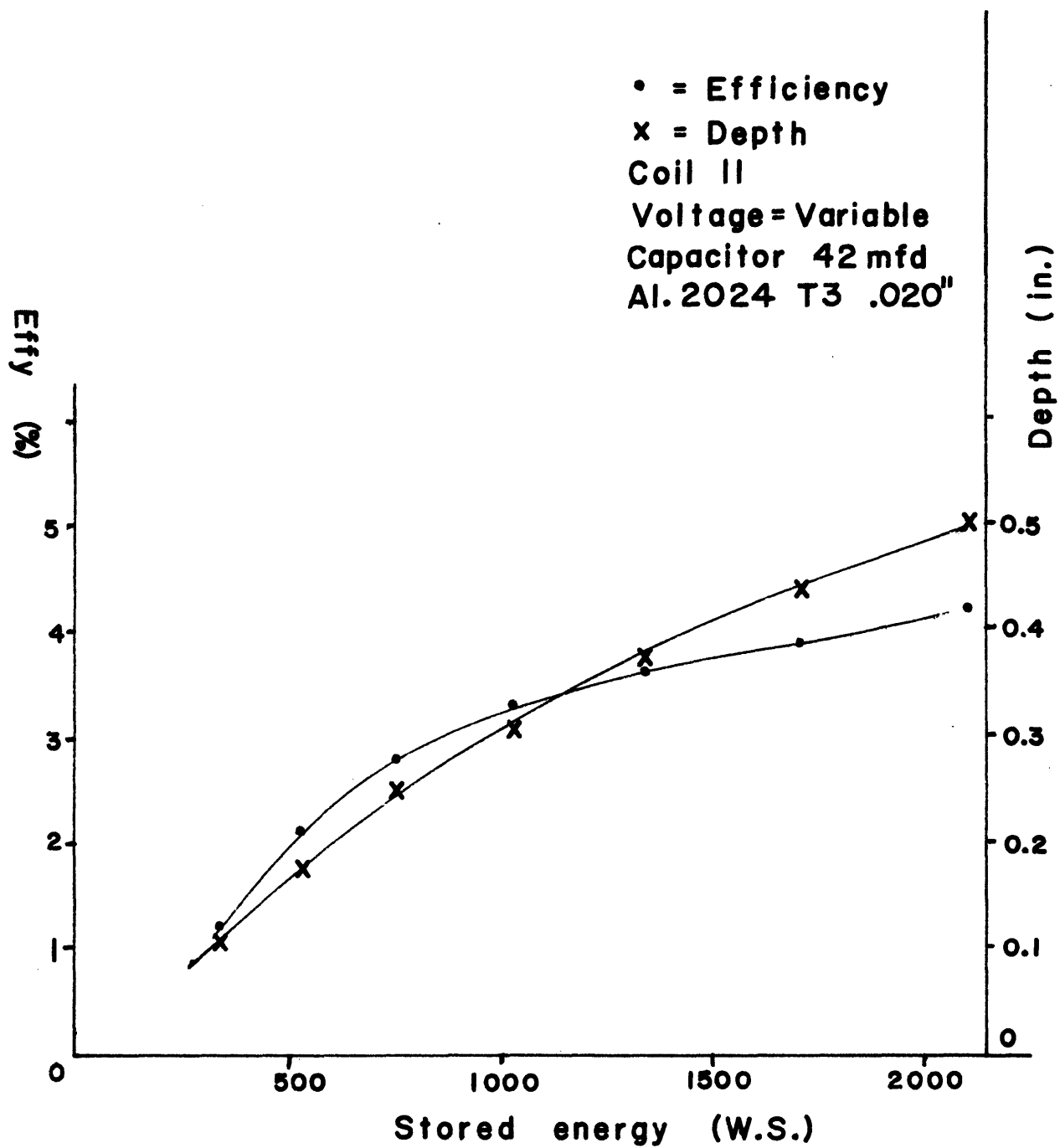


Fig. 22 Experiment V

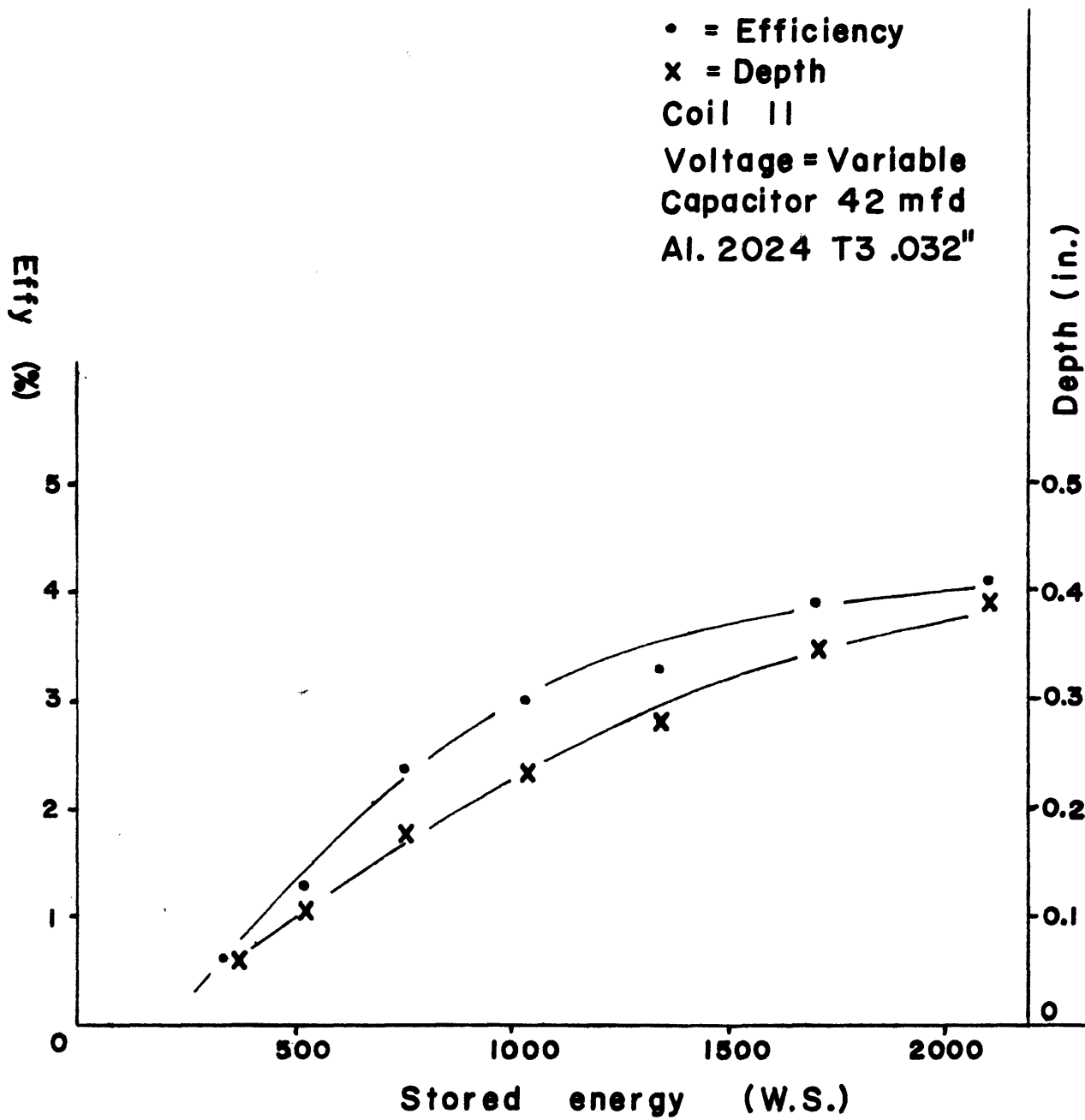


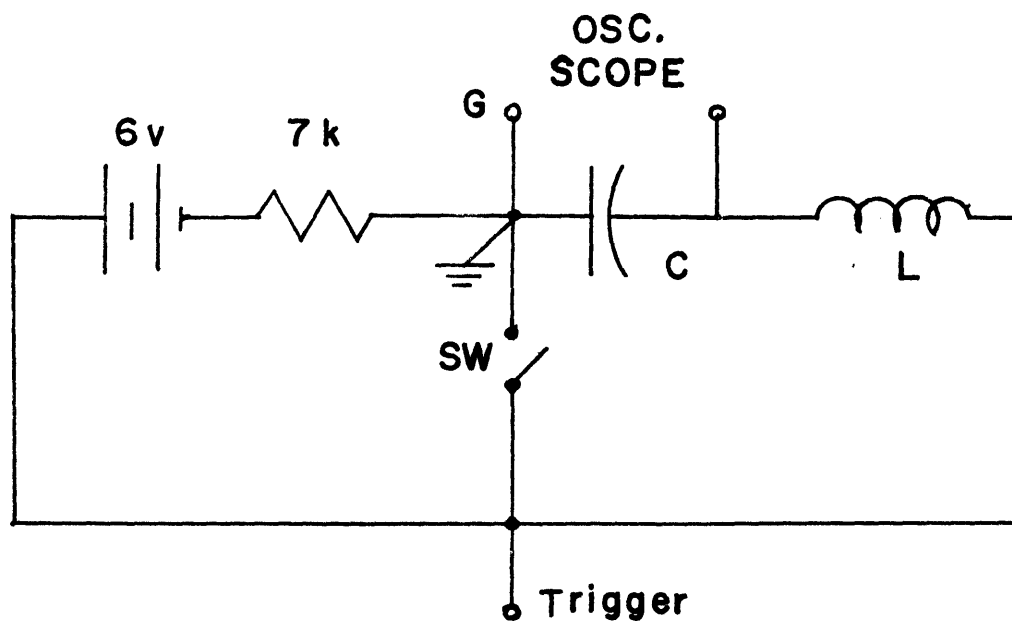
Fig. 23 Experiment VI

The experimental data proves that the higher voltage of the power supply is most effective for magnetic forming. When the voltage of power supply is constant, the increase of the capacitor bank over the certain amount, in this experiment, about 2000 Joule and 4 kv, doesn't improve the efficiency and is not effective for magnetic forming. The fixed capacitor and coil (inductance) determines the circuit parameters and the higher voltage makes the higher current changing rate which is very effective to induce higher magnetic flux, and the higher amplitude.

3-3. The observation of the oscillation at the time of discharge.

Instead of the actual high voltage system, a simulated circuit was used. Figure 23 shows the schematic diagram for this observation of the transients. Pictures were taken of the transient of the voltage between the terminals of capacitor, using the oscilloscope. The operation is as follows:

The switch is normally open. The energy of battery is stored in the capacitor. When the switch is closed, the stored energy of the capacitor is dissipated through the coil. The usual switch bounces at the make or break. We must use the no-bouncing switch, the special micro switch



C = Actual discharge capacitor 166 mfd

L = Coil II

SW = No bouncing switch

Fig.24 Observation of the transients

or Mercury Wetted Contact Relay (C. P. Clare & Co., Chicago).

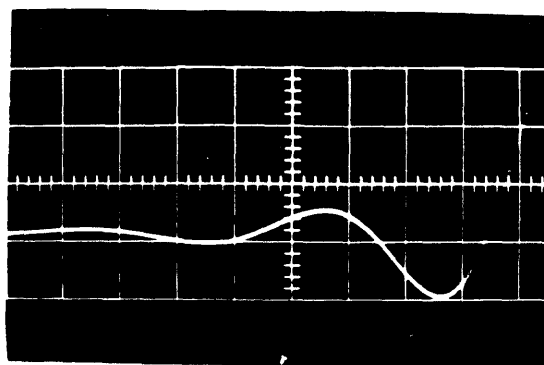
Observation I: Coil II without work-piece.

Fig. 24 shows the transient.

Observation II: Coil II with work-piece.

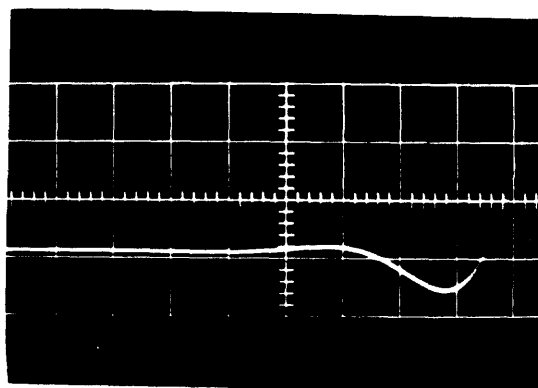
Fig. 25 shows the damping effect
of work-piece.

From the pictures, the effective total resistance of the system is recognized to be high and the voltage oscillates a few times at the instance of discharge. The period of the transient was about 400 micro-second, when the Coil II and capacitor 166 mfd were used. The inductance at 1 kc of the Coil II is about 15 micro-henry and $Q = 7.1$ or effective resistance .013 ohm.



Note = 2 v/division, 100 micro sec/division
without work piece

Fig.25 Observation I



Note = 2 v/division, 100 micro sec/division
with work piece

Fig.26 Observation II

Chapter Four: The utility and feasibility of Magnetic Forming

4-1. The distinguishing features of Magnetic Forming.

- (1) Only a female die is necessary and sometimes in swaging and tube-expanding operation, the die is not used.
- (2) A conductive material must be used for magnetic forming, otherwise the high resistive materials need another driving conductive material.
- (3) Swaging operations and the expansion of cylindrical components shall be difficult by the conventional method.
- (4) Magnetic forming is a high energy rate metal forming.
- (5) The system is dangerous under operation, because the power supply voltage is high and substantial energy is stored in the capacitor.
- (6) No transmitting medium is necessary. Magnetic forming is conducted in air.
- (7) No moving parts.
- (8) The easily adjustable control makes it possible to select the exact amount of force needed for the particular job.
- (9) Magnetic forming can speed up conventional operations and cuts production costs. "Magneform" pamphlet reports 600 individual operations per hour. The main factor which limits the maximum operations per hour is the charging time

of the capacitor bank (or the time constant).

(10) Magnetic forming will operate through thermal or electric insulating coatings.

(11) Easily interchangeable coils permit operations to be changed quickly, thus minimizing set-up time.

(Cf. Bibliography 10)

4-2. Possible uses of Magnetic Forming.

(1) Expanding.

The expansion of the cylindrical components can be performed. (Cf. Bibliography 2 and 5). The forming materials are assumed to be conductive. If the forming material is not conductive or of high resistive like steel, we can use another driving conductive material attached to it.

(2) Compression.

This means the swaging operation and assembly. Assembling metal fittings on ceramic insulators, etc., are reported by General Atomic Division, General Dynamics (Bibliography 10 and 11). Precise cylindrical shapes can be made, using die.

(3) Pressing and forming flat sheets.

Coining, shearing and forming and blanking are the useful operations of magnetic forming. Lettering (embossing) was carried out.

(4) Punching.

Magnetic force instead of mechanical force is possible for the punching operation which is suggested by Prof. Cook. This is the problem of the further investigation.

The thick Aluminum sheet is to be used and is connected directly to the punching die. In this case, the size of the coil which drives the Aluminum sheet like Sonar Transducer is not limited and can be made big enough. Figure 27 shows the schematic diagram. This method offers the advantage that the punched circle pieces are available for other purposes.

(5) Two pieces at the same time.

If the excess energy is available, both sides of the coil are possible for magnetic forming of flat metal.

4-3. The cost of this method.

The commercial machine is already available by General Dynamics, General Atomic Division. According to Rudel Machinery Company located at 531 Statler Building, Boston 16, Mass., the representative of General Atomic in the Boston area, "Magneform" (Trademark, General Dynamics Corporation) is priced \$15,000/unit (April, 1963). This includes the coils and necessary attachments.

On the other hand, the price of the units of Sonar

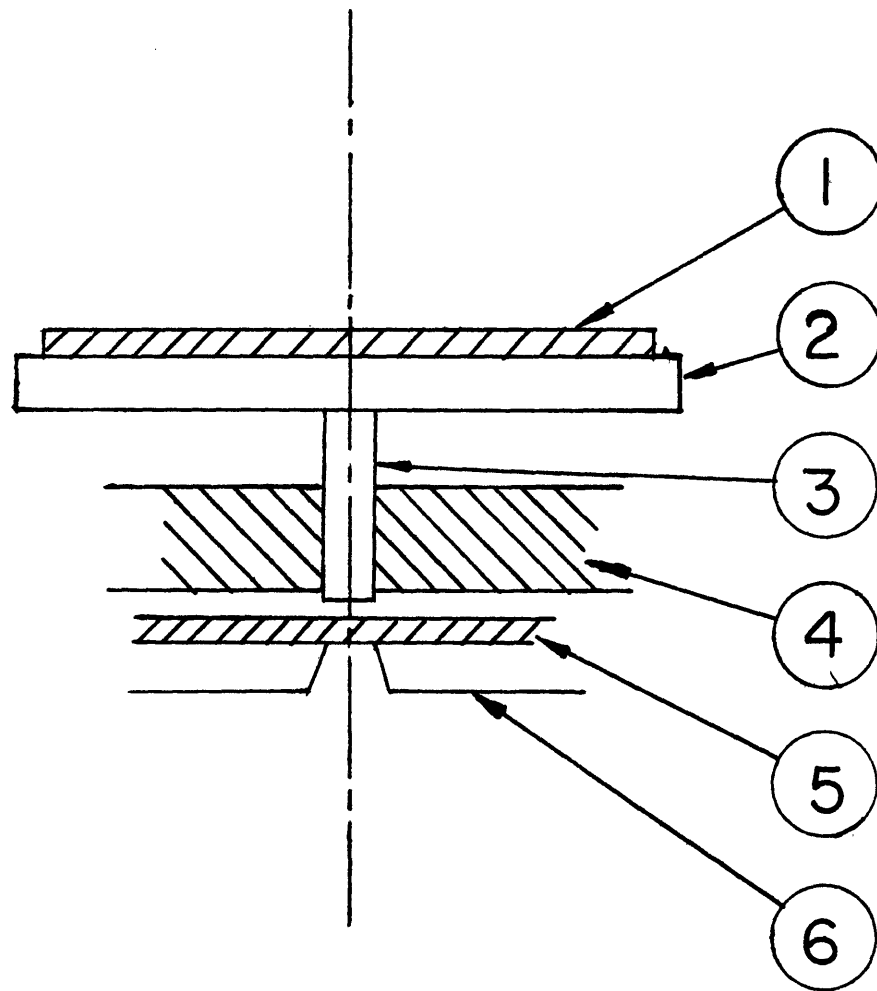


Fig. 27 Punching 1. Coil 2. Aluminum plate

3. Guide 4. Male punching die 5. Work piece

6. Female punching die

Transducer was investigated at Edgerton, Germeshausen and Grier.

1. Trigger Unit + 1000 WS banks	\$1,985.00
2. Power Supply	\$1,340.00
3. 2000 WS banks \$1,100 each,	
4000 WS	\$2,200.00
Total 5000 WS Unit	\$5,525.00

In this case, the coils are not included. It will be estimated that one watt-second is one dollar, and the coil-making needs considerable manual labor. It must take time to develop further utility. The capacitor's life is very long, and normal discharging operations are many times possible. The statement of Prof. Simon Foner and Prof. Henry H. Kolm in their paper (Bibliography 1) proves these things.

APPENDIX I. The definitions of terms.

The terms of mechanics of solids are not familiar to Electrical Engineers. It might be helpful to explain the terms.

- (1) A ductile material or structure is defined as one for which the plastic deformation before fracture is much greater than the elastic deformation.
- (2) Elastic deformation is defined as the deformation that disappears on release of load.
- (3) Plastic deformation is defined as the deformation which depends on the applied load, is independent of time, and remains on release of load.
- (4) Strain-hardening is termed the increase in the load required for further plastic deformation.
- (5) Yield strength is the stress required to produce a certain arbitrary plastic deformation. The yield strength is determined by drawing through the point on the abscissa corresponding to the arbitrary plastic strain, usually 0.2 per cent, a line which is parallel to the initial tangent to the stress-strain curve; the intersection of this line with the stress-strain curve defines the yield strength.
- (6) Brittle fracture stress is termed with the brittle materials.

(7) The true stress is termed with the intensity of load per unit of actual area.

The engineering stress is termed with the intensity load per unit of original area.

(8) The engineering strain

$$\epsilon_x = \frac{\Delta L}{L_0} = \frac{L_f - L_0}{L_0}$$

(Bibliography 12)

APPENDIX II. Tensile Test of Test Pieces.

Tensile Test was made for Aluminum 2024 T3 .020" and .032" thickness, using Housfield Tensometer manufactured by Tensometer Limited, 81 Morland Road, Croydon, made in England.

(1) .020" thickness.

$$\text{Elongation per cent} = \frac{.35 \times 100}{2} = 17.5\%.$$

$$\text{Max. Stress} = \frac{.305}{.5 \times .021} = 29.1 \text{ tons/in}^2.$$

Strain(x100%)	Stress(lb/in ²)
.00020	2133.33
.00040	4266.66
.00060	6400.00
.00077	8533.33
.00100	10666.66
.00120	12800.00
.00140	14933.33
.00160	17066.66
.00180	19200.00
.00202	21333.33
.002225	23466.66
.00245	25600.00
.00267	27733.33
.00287	29866.66
.003125	32000.00
.003375	34133.33
.003725	36266.66
.0041	38400.00
.0046	40533.33
.0053	42666.66
.0066	44800.00
.0072	45866.66
.00845	46933.33
.0097	48000.00
.01095	49066.66

(continued)

Strain(x100%)	Stress(lb/in ²)
.0122	49706.66
.01345	50133.33
.0147	50773.33
.01595	51200.00
.0172	51626.66
.01845	52053.33
.0197	52266.66
.0222	52906.66
.0247	53333.33
.0272	54400.00
.0297	54826.66
.0322	56533.33

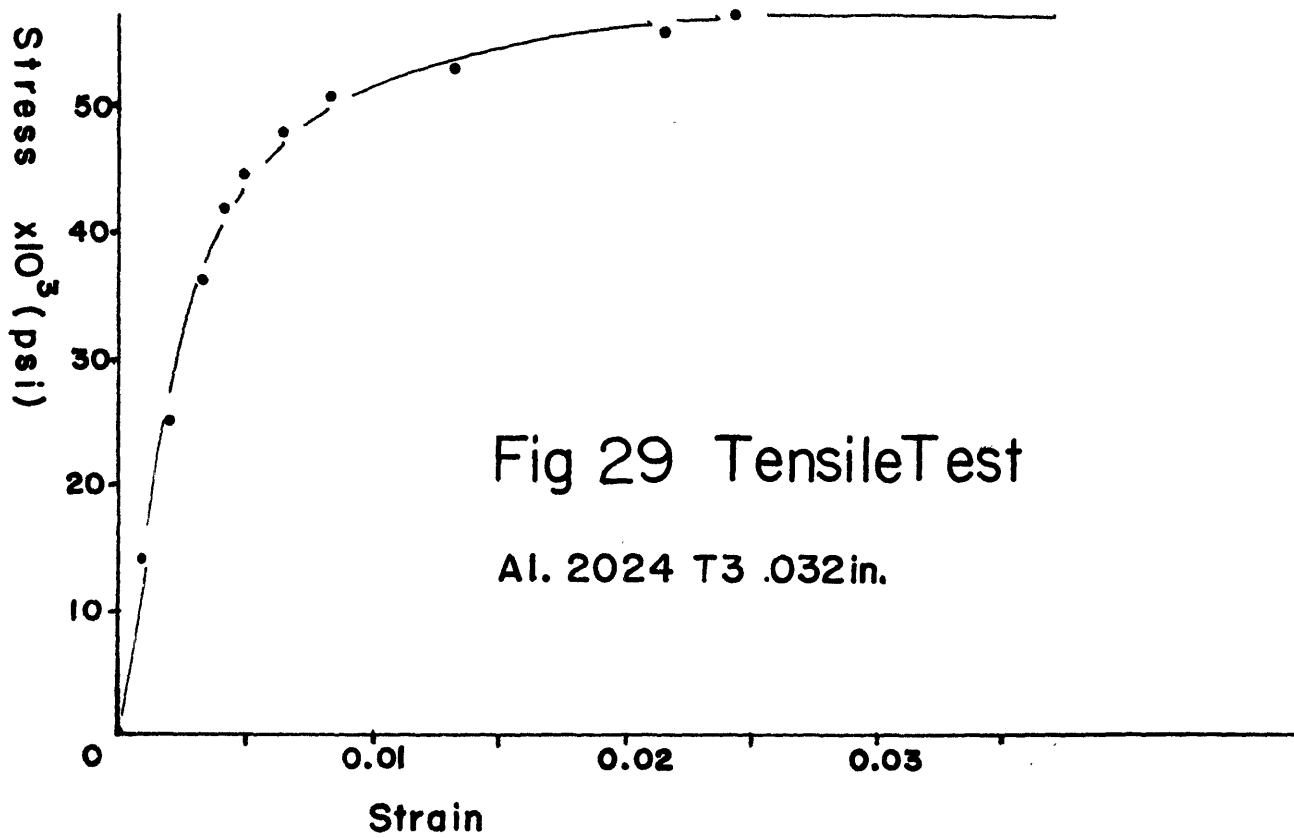
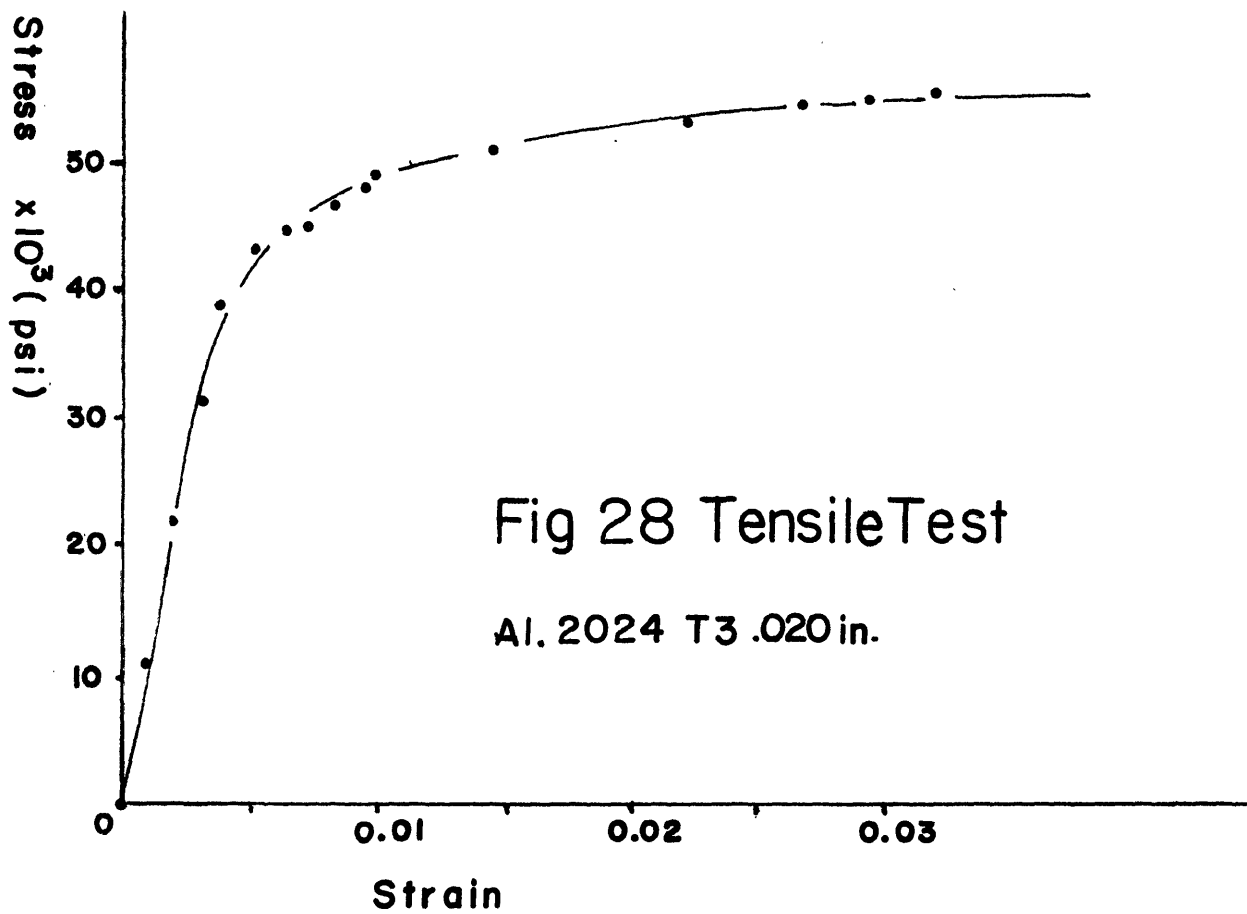
(2) .032" thickness.

$$\text{Elongation per cent} = \frac{.375 \times 100}{2} = 18.8 \%$$

$$\text{Max. Stress} = \frac{.49}{.5 \times .032} = 30.6 \text{ tons/in}^2.$$

Strain(x100%)	Stress(lb/in ²)
.00045	7000
.00075	10500
.0011	14000
.00145	17500
.0018	21000
.0019	22400
.0022	25200
.00245	28000
.0027	30800
.00335	36400
.0038	39200
.00425	42000
.005	44800
.0063	47600
.0087	50400
.01345	53200
.0217	56000
.02245	57400

These results were plotted in Figs. 28 and 29.



APPENDIX III. Comment on the improvement of coil.

As the reader sees the distribution of the magnetic field intensity for one turn coil (Fig. 2), the edges of the coil are very effective for magnetic forming. This conclusion deduced from the results of the calculation of field intensity, was used to improve the coil (see Fig. 11, the experiments proved that Coil II was better than Coil I, Cf. Fig. 18 - 21).

Even if many turns were wound together, each turn would work independently, as far as Magnetic Forming is concerned. In the case of Chapter Four, 4-2, (5), we can use the double-layer coil for taking out the lead and reinforcing the magnetic field.

BIBLIOGRAPHY

1. "Coils for the Production of High-Intensity Pulsed Magnetic Fields," Simon Foner and Henry H. Kolm, The Review of Scientific Instruments, v 28, n10, Oct., 1961, p.799-807.
2. "Magnetic Forming", William A. Wilson and R. J. Schwinghamer, Industrial Research, Feb., 1963, p.25-28.
3. "What Magnetic Forming Can Do," A. P. Langlois, Am. Mach. Metalworking Mfg., v 105 n7, April 3, 1961, p.99-102.
See also Tool & Mfg. Engr. v 46 n6 May 1961, p.105-108.
Machy (N.Y.) v 67 n11 July 1961, p.86-91.
4. "Metalworking Report," AM/MM v 103, n24 November 16, 1959, p.2-3.
5. "Magnetic-Pulse Forming," D. E. Brower. SAE -- paper 479B for meeting Jan. 8-12, 1962,
See also SAE -- J. v 70 n2 Feb. 1962, p.38-40.
6. "Experimental Pinch Stabilization with Large Axial Magnetic Field," D. F. Brower, R. E. Dunaway, J. H. Malmberg, C. L. Oxley, M. Stearns, D. W. Kerst, F. R. Scott, S. P. Cumingham and R. G. Tuckfield, Jr. Proceedings of the Second United Nations International Conference on the Peaceful Uses of Atomic Energy 1958, vol 32 P/352 USA, p.110-112.
7. "Joint General Atomic - TAERF Fusion Program," D. W. Kerst, Proceedings of the Second United Nations International Conference on the Peaceful Uses of Atomic Energy, 1958, vol 32 P/1062 USA, p.106-109.
8. "Magnetic Forming!," AM. Mach. Metalworking Mfg. v 104 n20, Oct. 3, 1960, p.95-96.
9. The phenomenal theory of electro-magnetism, Setsuzo Takeyama, Maruzen Co., Tokyo, Japan, 1958.

10. Magneform (the Pamphlet), Magneform Sales, Dept. 203, General Atomic Division, General Dynamics Corporation, P.O. Box 608, San Diego 12, California.
11. MAGNEFORM Application Data, No. 1021, 1022, 1023, and 1026, General Atomic Division, General Dynamics Corporation, P.O. Box 608, San Diego 12, California.
12. An introduction to the mechanics of solids, edited by Stephen H. Crandall and Norman C. Dahl, McGraw-Hill Book Company, Inc. 1959. Chapters 4 & 5.
13. An investigation into the feasibility of the electro spark hydraulic forming processes, Jonathan Gestetner, S.B. Thesis of Mechanical Engineering at M.I.T., January, 1960.